UNIVERSITÀ DEGLI STUDI DI PARMA

Dottorato di ricerca in

Farmacologia e Tossicologia Sperimentali

Ciclo XXVI

DEVELOPMENT OF NEW RAC1 INHIBITORS AS POTENTIAL PHARMACOLOGICAL AGENTS FOR THE TREATMENT OF CARDIOVASCULAR DISEASES: FROM IDENTIFICATION TO *IN VIVO* STUDY

Tesi di Dottorato di:
Sergio Kevin Bernini

Coordinatore del dottorato:
Chiar.ma Prof.ssa Elisabetta Barocelli

Tutore:
Dott. Nicola Ferri
Chiar.mo Prof. Alberto Corsini

Triennio Accademico 2011-2013

Introduction

Heart hypertrophy: pathogenesis and new potential pharmacological targets

Cardiac hypertrophy is an adaptive response to pressure or volume stress, mutations of sarcomeric (or other) proteins, or loss of contractile mass from prior infarction. Hypertrophic growth accompanies many forms of heart diseases like ischemic disease, hypertension, heart failure, and valvular disease[12]. In these types of cardiac pathology, pressure overload–induced concentric hypertrophy is believed to have a compensatory function by diminishing wall stress and oxygen consumption. Moreover, ventricular hypertrophy is associated with significantly increased risk of heart failure and malignant arrhythmia[34].

Hypertrophic transformation of the heart is subdivided into 3 steps[5]: (1) developing hypertrophy, with load exceeds output, (2) compensatory hypertrophy, in which the workload/mass ratio is normalized and resting cardiac output is maintained, and (3) overt heart failure, with ventricular dilation and progressive declines in cardiac output despite continuous activation of the hypertrophic program[6]. The late-phase "remodeling" process that leads to failure is associated with functional perturbations of cellular Ca^{2+} homeostasis and ionic currents[7,8], which contribute to an adverse prognosis by predisposing to ventricular dysfunction and malignant arrhythmia. Significant morphological changes include increased rates of apoptosis[9], fibrosis, and chamber dilation.

The cellular hypertrophic response is an important adaptive process in the

cardiomyocites in response to various extracellular stimuli like mechanical stress, cytokines, and growth factors, moreover it is characterized by an increase in cell volume, the assembly of contractile proteins into reorganized sarcomeric units.

At the molecular level, these changes in cellular phenotype are accompanied by reinduction of the so-called fetal gene program, because patterns of gene expression mimic those seen during embryonic development like the reactivation of atrial natriuretic factor (ANF) and brain natriuretic peptide (BNP), for this reason, both peptides are used as prognostic and diagnostic markers in many cardiovascular abnormalities such as hypertension, heart failure, left ventricular diastolic dysfunction, valvular stenosis and coronary artery disease[10].

During the heart hypertrophy development we can distinguish two different phenotypes: (1) concentric hypertrophy due to pressure overload, characterized by parallel addition of sarcomeres and lateral growth of individual cardiomyocytes, and (2) eccentric hypertrophy due to volume overload or prior infarction, characterized by addition of sarcomeres in series and longitudinal cell growth[11].

Experimental evedence suggest that the renin–angiotensin system (RAS) and its effector peptide, angiotensin II (Ang II), are involved in the pathophysiology of cardiac hypertrophy and failure. All the components required for Ang II production are present in the heart, and cardiac Ang II formation appears to be regulated independent from the circulating RAS. In animal models and in

patients with heart failure, the cardiac RAS is activated and, probably, local Ang II formation is enhanced. Several cardiac cell types express Ang II type 1 (AT) and/or type 2 (AT)-receptors and represent potential targets for Ang II-mediated effects.

The increasing of reactive oxygen species (ROS) production is implicated in the development of cellular hypertrophy and remodeling, at least in part, through activation of redox-sensitive protein kinases such as the mitogen-activated protein kinase (MAPK) superfamily. The transition from compensated pressure-overload LVH to heart failure is related with increased oxidative stress, which may promote myocyte apoptosis and necrosis. Several key proteins involved in excitation-contraction coupling, such as sarcolemmal ion channels and exchangers and sarcoplasmic reticulum calcium release channels, can undergo redox-sensitive alterations in activity, which contributes to myocardial contractile dysfunction. ROS also has indirect effects resulting from increased inactivation of NO and consequent generation of peroxynitrite, for example, coronary vascular endothelial dysfunction and peroxynitrite-induced inhibition of myocardial respiration.

Role of NADPH oxidase in the production of reactive oxygen spieces and its implication in cardiovascular diseases.

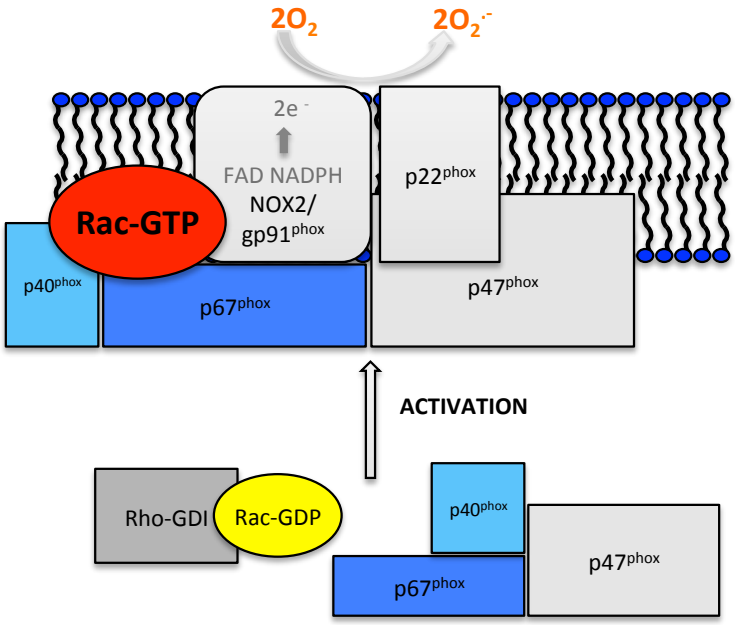

Figure1: Role of NADPH oxidase in the production of reactive oxygen spieces and its implication in cardiovascular diseases. Activation of the NADPH oxidase requires the assembly of a multimolecular complex at the plasma membrane consisting of two integral membrane proteins, gp91phox and p22phox, and two cytosolic proteins, p67phox and p47phox. Rac1 interacted directly with p67phox in a GTP-dependent manner.

NAD(P)H oxidase is a multi-subunit enzyme that catalyzes $\cdot O_2^-$ production by the 1-electron reduction of O_2 using NADPH or NADH [hence the parentheses in NAD(P)H] as the electron donor: $2O_2$ + NAD(P)H give $2 \cdot O_2^-$ +$NAD(P)^+ + H^+$.

NAD(P)H has five subunits: p47phox ("phox" stands for phagocyte oxidase), p67phox, p40phox, p22phox, and the catalytic subunit gp91phox (also termed "Nox2")[12,13]. In unstimulated cells, p47phox, p67phox, and p40phox exist in the

cytosol, whereas p22phox and gp91phox are in the membrane, where they occur as a heterodimeric flavoprotein, cytochrome b558. On stimulation, p47phox becomes phosphorylated and the cytosolic subunits form a complex that translocates to the membrane, where it associates with cyto-chrome b558 to assemble the active oxidase, which transfers electrons from the substrate to O_2, forming $\cdot O_2^-$ [14]. A second important event required for NADPH oxidase activity is Rac activation and membrane translocation. The mechanisms by which Rac regulates the NADPH oxidase are incompletely understood. In cell-free oxidase reconstitution assays, the Rac-GTP active form is essential for high level superoxide production[15,16]. Rac-GTP binds the N-terminal TPR (tetratrico repeat) region of p67phox and may also interact directly with the flavocytochrome in the assembled oxidase complex[17–22].

Seven isoforms of NADPH oxidase have been described in mammals. Each of these isoforms comprises a core catalytic subunit, the NADPH oxidase (NOX) and dual oxidase (DUOX) subunits, and up to five regulatory subunits. These regulatory subunits have important roles in: maturation and expression of the NOX and DUOX subunits in biological membranes, (ie, p22phox, DUOX activator 1, and DUOX activator 2), in enzyme activation (p67phox and NOX activator 1), and in spatial organization of the various components of the enzyme complex (p47phox, NOX organizer 1, and p40phox).

The biological roles of NADPH oxidase make it an interesting therapeutic target, because the ROS-generating activity of vascular smooth muscle cells and endothelial NADPH oxidases is increased by stimuli such as angiotensin II,

tumor necrosis factor-α, growth factors and cyclical load. Vascular NADPH oxidases are implicated in the development of angiotensinII–induced vascular smooth muscle cells hypertrophy, hypertension, endothelial dysfunction, and atherosclerosis. However, further investigations are needed to clarify the different roles of the NADPH oxidase isoforms and their participation in signaling pathways, in addition to the requirement for developing isoform-specific inhibitors.

The oxidative stress damages the proteins, lipids and DNA, causing cellular dysfunction[23]. In particular, an excess of $O2^{\cdot-}$ may decrease nitric oxide (NO) availability, leading to endothelial dysfunction and a decrease in endothelium-dependent vasodilation[24]. Additionally, oxidative modification of proteins may result in the formation of nitrotyrosine, which represents a powerful and autonomous marker of cardiovascular diseases.

Furthermore, $O2^{\cdot-}$ is implicated in the generation of oxidized LDL (oxLDL), a key initiator of atherosclerosis[25].

Rac1 has been reported to be a key regulator of oxidative stress through its co-regulatory effects on both NO synthase and NOX, moreover Rac1 performs many important biological functions in cells, but perhaps the most unique function is its ability to bind and activate the NOX complex. Upon enzyme activation, translocation as well as assembly of the cytosolic subunits to the membrane subunits take place. In the activated enzyme complex, the catalytic subunit acts as an electron transport system that utilizes NADPH as an electron donor to transfer electrons to molecular oxygen, leading to the formation of

$O2^{\cdot-}$ [26,27].

In various studies the, upregulation of Rac1 and p47phox membrane protein expression as well as increased Rac1-GTPase activity may resemble the underlying mechanisms for increased oxidase activity, in particular, Rac1-GTPase activation seems to play a main role in the initiation of cardiac hypertrophy linking NOX-related ROS production to the hypertrophic signalling cascade.

BNP and ANF: biomarkers for heart development and disease

The heart of mammals expresses atrial natriuretic factor (ANF, ANP, a-type natriuretic peptide) and brain natriuretic peptide (BNP, b-type natriuretic peptide). Both proteins and their encoding genes have been studied extensively[28,29] for their various physiological functions and expression in different organs.

Their main effects are to lower blood volume, reducing cardiac output and systemic blood pressure.

Ventricular expression of the genes for ANF and BNP is downregulated after birth, while their levels significantly increase during heart hypertrophy and heart failure.

ANF was the first natriuretic peptide to be identified, when it was shown to increase natriuresis, diuresis and vasodilation[30], moreover the spectrum of action was not limited to cardiovascular and renal systems. Receptors for ANF were identified in different organs including the kidney, lung, liver, adrenal

cortex, and the small intestines, where it could regulate salt and water balance as well[31], also ANF receptors[31] as well as bioactive peptide were also found in the brain[32,33,34], where contains another NP, therefore called BNP[35].

In the brain NPs inhibit the release of adrenocorticotropic hormone, thereby decreasing aldosterone release and enhancing natriuresis. Furthermore, the ANF-ergic neurons inhibit arginine vasopressin release leading to diuresis[36]. Therefore, NPs expressed in the brain also serve to maintain optimal liquid homeostasis. Although BNP was isolated from the brain, it is predominantly expressed in the heart ventricles and mimics the pharmacological activity of ANF in regulation of blood pressure, ANF and BNP proteins showed a similar structure.

ANF and BNP are stored in the same secretory granules in the atria therefore during cardiac cell stress, they are rapidly released from pre-stored granules[37], and their concentration in the blood is expected to rise simultaneously and to the same grade.

Indeed, studies show synchronous elevation of plasma ANF and BNP during the time-course of acute volume or pressure overload[38,39] as well as presence of both elevated ANF and BNP in chronic models of hypertension.

The induction of NP levels and gene expression in response to heart diseases were performed both in short-term experiments and in a long term experiments: Short-term experiments were performed with isolated atria or ventricles to estimate secretion of NPs in minutes after stimulation, which showed that both ANF and BNP were acutely secreted with a peak at about 20–

30 min after atrial pacing[40,41] and after 1–5 min after ventricular stimulation[42]. These results indicate that atrial and ventricular myocytes rapidly respond to stress.

In a long term experiments with chronic overload revealed some differences in atrial and ventricular secretion of the NPs: in spontaneously hypertensive rats (SHR) the secretion of ANF from the overloaded left ventricle was accompanied by the decrease in ventricular concentration of immunoreactive ANF, while atrial protein concentration was not changed compared to the control rats. In vitro studies with the isolated hearts showed that hypertensive ventricles contributed 28% of the total ANF released, while normotensive ventricles contributed only 8%. These experiments suggest that excess ANF is released from the ventricular stores[43]. However, in the settings of right ventricular hypertension, right atrial content as well as whole heart content of ANF was decreased[44], indicating atrial secretion of ANF. The difference can be explained by the differences in complex regulation of NPs release from the secretory granules and their de novo synthesis from an increased pool of mRNA.

Temporal regulation of ANF and BNP enhanced expression is also different in various conditions of cardiac disorders. After myocardial infarction, induced by isoproterenol injections in rats, BNF mRNA was upregulated in both ventricles at 18 h after injection, whereas ANF mRNA level gradually increased until significant levels 3 days after isoproterenol administration[45]. The same trend was observed in rats with aortocaval shunt, where both ANF and BNP plasma

levels were steady elevated at 1 day and 7 days after surgery. Expression of BNF was induced only at 1 day after volume overload, but upregulation of ANF mRNA followed that of BNP only in 7 days after surgery[46,47]. Acute ventricular overload after MI[48,49] , hypertension[50] and volume overload[51] leads to rapid and sometimes transient upregulation of BNP mRNA in the affected ventricular myocardium, whereas ANF upregulation follows BNP at later time points.

The mechanisms of ANF and BNP gene expression are regulated by various stimuli like mechanical stress, growth factors and G protein-coupled receptors. The expression of ANF and BNP in mechanical stress were studied in isolated cardiomyocytes, and atrial and ventricular preparation to separate the response of cardiomyocytes to strain from systemic response induced by neurohumoral factors. Mechanical stretch induces ANF, BNP and skeletal alpha-actin mRNA expression in neonatal ventricular cardiomyocytes[36] and atrial preparations[52,53,54]. The signal from mechanically-strained extracellular matrix propagates through the integrins and a cascade of intracellular kinases to activate p38 MAP kinase and NF-kB[55,56] and promote binding of the latter to shear stress-responsive elements (SSREs) in the BNP promoter. In parallel with direct activation of BNP through p38 MAPK, mechanical strain stimulated synthesis of AngII and ET-1, which induced the ERK-signaling pathway acting on the BNP promoter[57,58].

Several neurohumoral factors are involved in the hypertrophy response of the heart, including activation expression and secretion of ANF and BNP. AngII is the main effector of the renin–angiotensin system, and was found to be

involved in hypertrophy remodeling through activation of AT1 receptors on cardiomyocytes, fibroblasts and smooth muscle cells within the heart, which triggers G protein-coupled and non-G protein-coupled signaling pathways including MAP kinases (ERK 1/2, JNK, p38MAPK), receptor tyrosine kinases (PDGF, EGFR, insulin receptor), non-receptor tyrosine kinases (Src, JAK/STAT, FAK) and reactive oxygen species.

The production of TGFα stimulated by AngII in cardiac myocytes and fibroblasts[59], thereby influencing the regulation of NPs through TGFα-GATA4 pathway[60].

Analysis of ANF expression and regulation during development of the heart has provided important mechanistic insights into the development of the chamber myocardium and the conduction system of the heart.

In conclusion analysis of transcriptional regulation of ANF and BNP in different animal models of cardiomyopathy demonstrated the use of NPs in biomedical research to assess hypertrophic response in the development of HF, which is in agreement with their extensive application as biomarkers in a broad range of cardiovascular diseases in clinical practice.

Small G-proteins: activation and biological roles

Rho GTPases of the Ras superfamily are involved in the regulation of multiple cell functions and have been implicated in the pathogenesis of cardiovascular diseases like heart hypertrophy and atherosclerosis. The Rho family comprises 22 genes encoding at least 25 proteins in humans, including the Rho, Rac, and

Cdc42, proteins playing a fundamental role in cell biology. Two regulatory steps are required for the full activation of Rho proteins, the isoprenylation process for the translocation in membrane and the binding to the GTP[61,62] (Figure2).

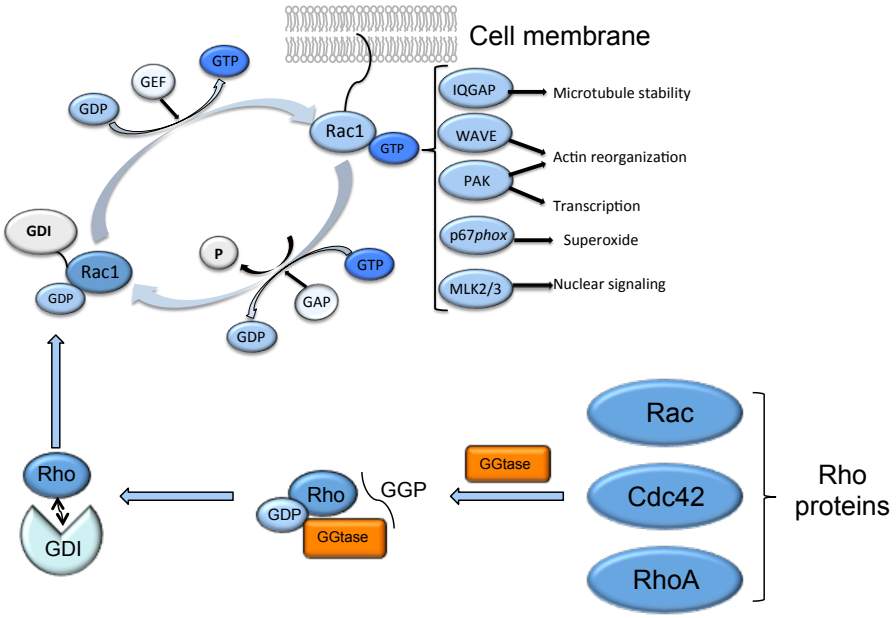

Figure2: Molecular mechanism for small G-proteins activation. Two main regulatory steps are required for the full activation of Rac protein, the isoprenylation process catalyzed by the geranylgeranyl transferase I (GGTase) required for the ligand to the cytoplasmatic membrane and the binding to the GTP. In cytoplasmic membrane the activation state of Rho proteins depends on the release of GDP and the binding with GTP. This cycling is finely regulated by three groups of proteins: the guanine nucleotide exchange factors (GEFs) as activators, and the GTPase activating proteins (GAPs) and GDP dissociation inhibitors (GDIs) as negative regulators.

The isoprenilation step, in common with all Rho proteins, is catalyzed by the geranylgeranyl transferase I (GGTase I) that covalently transfer the isoprenoid geranylgeranyl from prenyl donor geranylgeranyldiphosphate (GGPP) to a cysteine residue of Rho proteins containing a C-terminal CAAX motif, in which

C is the cysteine that is geranylgeranylated.

In membrane Rho family members bind GTP, and most exhibit GTPase activity and cycle between an inactive GDP-bound form and an active GTP-bound form. This cycling is finely regulated by three groups of proteins: the guanine nucleotide exchange factors (GEFs) as activators; the GTPase activating proteins (GAPs) and GDP dissociation inhibitors (GDIs) as negative regulators. When bound to GTP, Rho GTPases interact with their downstream effectors, which include protein kinases, regulators of actin polymerization, and other proteins with adaptor functions. The selective interaction of the different Rho GTPases with a variety of effectors determines the final outcome of their activation.

The best characterized function of Rho family proteins is the regulation of the actin cytoskeleton, with RhoA involved in the formation of actin stress fibers and focal adhesion complexes, Rac1 in facilitating actin polymerization at the cell periphery to generate protrusive actin-rich lamellipodia and membrane ruffling, and Cdc42 in the formation of filopodia[63]. From these evidences it has been hypothesized a direct involvement of the Rho proteins in the fibroproliferative and hypertrophic responses associated with cardiovascular diseases, such as atherosclerosis and cardiac hypertrophy.

In a study of pathway-based genome-wide association analysis has recently identified Rac1 as one of the biologically important gene in coronary heart diseases. The role of the small GTPase Rac1 in cardiac hypertrophy and atherosclerosis has also been documented in clinical studies with the HMG-CoA

reductase inhibitors, and in *in vitro* and *in vivo* settings using transgenic and knock-out mice. Thus, Rac1 has emerged as a new possible pharmacological target for the treatment of cardiovascular diseases.

Small G-proteins and heart hypertrophy

The low-molecular-weight or small GTPase superfamily consists of more than 100 members. They are divided into 5 subfamilies: (1) Ras, (2) Rho/Rac/cdc42, (3) Arf/Sar1, (4) Rab, and (5) Ran. All monomeric G proteins are characterized for their specificity for regulation of cell structure[64].

From this family, Ras, was the first small GTPase protein linked to cardiac remodeling, it is the most extensively characterized of the family in the myocardial setting[65].

In a second moment, the Rho/Rac/cdc42 family has received greatest attention for their actions in myocardial cells and, of the 20 known Rho family gene products, the most extensively characterized members for the myocardial signaling was Rac1 and RhoA.

The effects of RhoA and Rac1 on the actin cytoskeleton and cell morphology are mediated through stimulation of downstream effector kinases by the activated Rho-GTP proteins[66]. For RhoA, the best known effectors are Rho kinase (ROCK) and mammalian diaphanous (mDia)[67]. ROCK phosphorylates the myosin binding subunit of myosin light chain (MLC) phosphatase resulting in increased myosin phosphorylation and contraction[68]. The discovery of a role for RhoA- and ROCK- mediated myosin phosphorylation in vascular smooth

muscle contraction[68,69,70], the finding that RhoA activity is upregulated in hypertension and the demonstrated efficacy of the ROCK inhibitor Y-27632 in lowering blood pressure have convincingly demonstrated involvement of RhoA/ROCK signaling in hypertension[71,72,73]. RhoA and ROCK signaling pathways have also been implicated in cerebrovascular stroke and in vascular endothelial permeability.

The role of RhoA in vivo were studied from Several transgenic and knockout mouse models have been examined to delineate the role of RhoA signaling pathways in vivo. In work from Sah et al were generated transgenic mice in which constitutively activated (L63A) RhoA or wild-type RhoA were expressed in a cardiac specific manner through the α-MHC promoter[74]. Most founders and progeny of the activated RhoA lines did not survive to adulthood. Mice expressing wild-type RhoA also showed increased mortality, which was dependent on gene dose and modestly rescued by backcrossing into a C57 (versus Black Swiss) line to give 50% survival at approximately 3 months. surprisingly, these mice did not develop an obvious hypertrophic response. Although both ANF and α-MHC expression were increased, there was no significant increase in ventricular weight to tibial length, nor was there an increase in cardiomyocyte size. On the other hand, evidence of heart failure was seen in RhoA transgenics, with severe edema, ventricular chamber dilation, increased cardiac fibrosis, atrial enlargement, and decreased fractional shortening. It is not clear what underlies the failure of in vivo RhoA expression to mimic the in vitro hypertrophic phenotype, but effects on

postnatal development, compensatory responses, or the more prolonged duration of RhoA expression are possibilities. It is also notable that a recent study using animals in which the RhoA effector, ROCK1, was partially deleted (ROCK1 haploinsufficient mice) did not show decreased hypertrophy but rather decreased fibrosis[75]. Applying these data to the observations made with the cardiac RhoA transgenic mouse suggests the possibility that RhoA in cardiomyocytes could act through a ROCK-dependent paracrine pathway to alter cardiac fibroblast proliferation. Another striking observation made in the RhoA transgenic mice was that many developed atrial fibrillation and atrioventricular (AV) block, as well as severe bradycardia, with heart rates nearly half those of nontransgenic littermate controls[74]. Effects on the conduction system could reflect effects of RhoA in modulating the activity of cardiac ion channels.

However, is unclear whether the observed salutary effect of blocking RhoA/Rho kinase signaling reflects changes in the cardiomyocyte or is a consequence of more directly inhibiting fibroblast proliferation/migration or of attenuating local inflammatory responses. There is evidence that Rho can be activated in cardiac fibroblasts and affect their proliferation[76]. Indeed the study cited above using ROCK 1 haploinsufficient (-/+) mice supports the notion that a critical function for RhoA/ROCK1 could reside in the fibroblast where it mediates perivascular fibrosis induced by TAC, myocardial infarction, or Ang II. Determining whether acute activation of RhoA and ROCK signaling pathways within the myocyte serve protective or deleterious functions is critical to

understanding the utility, timing, and targets of inhibition of RhoA signaling.

For Rac1 activation two predominant effector response pathways lie downstream in cellular signaling: induction of cytoskeletal remodeling and formation of ROS. A diverse team of cytoskeletal remodeling proteins are influenced by Rac1 and referred to by acronyms or unintuitive abbreviations including WASP (Wiskott–Aldrich syndrome protein), WAVE (WASP with a V-domain), IQGAP (calmodulin-binding GTPase activating proteins), and PAK (p21-activated kinase)[77]. PAK shows homology to another kinase that binds to Rac1 named mixed lineage kinase 3 (MLK3) that, on activation, promotes the MEKK-SEK-JNK signaling cascade[78]. Our understanding of how cytoskeletal dynamics in the myocardium is regulated by this alphabet soup of factors is very rudimentary, but at least PAK has achieved visibility in regulation of contractility[79]. The cardiovascular literature is, in contrast, replete with examinations of ROS- mediated effects that can be triggered, at least in part, by Rac1 binding to p67 phox, leading to activation of the NADPH oxidase system. The subsequent generation of ROS, which cascades into multiple cardiovascular effects including hypertrophy, hypertension, atherosclerosis, chemotaxis, and platelet aggregation, has been recently summarized[80] and is considered elsewhere in this thematic series.

Studies using activated or dominant interfering mutants of RhoA or Rac1 have implicated these proteins in numerous pathways regulating gene expression. Among the earliest described effects of RhoA was its ability to elicit serum response element (SRE)-mediated transcriptional activation through a TCF-

independent, SRF-mediated pathway. In addition, RhoA has been implicated in transcriptional activation of AP-1,[81,82] GATA-4,[83] nuclear factor (NF)-κB,[84,85] and MEF2 pathways[86,87]. For Rac1, activation of MAPK kinase cascades upstream of c-Jun N-terminal kinase (JNK), and p38 elicits transcriptional changes. For example, regulation of target genes such as brain natriuretic peptide (BNP) or atrial natriuretic factor (ANF) are influenced by Rac1 activity. Thus, there are numerous potential pathways by which RhoA or Rac1 activation and signaling could contribute to the well-described alterations in gene expression associated with cardiomyocyte hypertrophy and remodeling.

Role of small G protein Rac in the heart hypertrophy

In vitro evidence

Experiments conducted by transfecting cardiomyocytes with a plasmid encoding for the constitutively active mutant of Rac1 (V12Rac1) documented a profound effect on sarcomeric reorganization, increase cell size, and induction of ANF expression, although the dominant-negative mutant of Rac (N17Rac) attenuates the morphological hypertrophy associated with phenylephrine stimulation[88]. Further investigations demonstrated that activation of Rac1 in response to phenylephrine and endothelin-1 contributes to the hypertrophic adaptation of cultured cardiomyocytes by modulating the ERK cascades[89]. Differently, in the stretch-induced hypertrophic response, Rac1 increases p38–MAPK activity and protein synthesis[90] (Figure3).

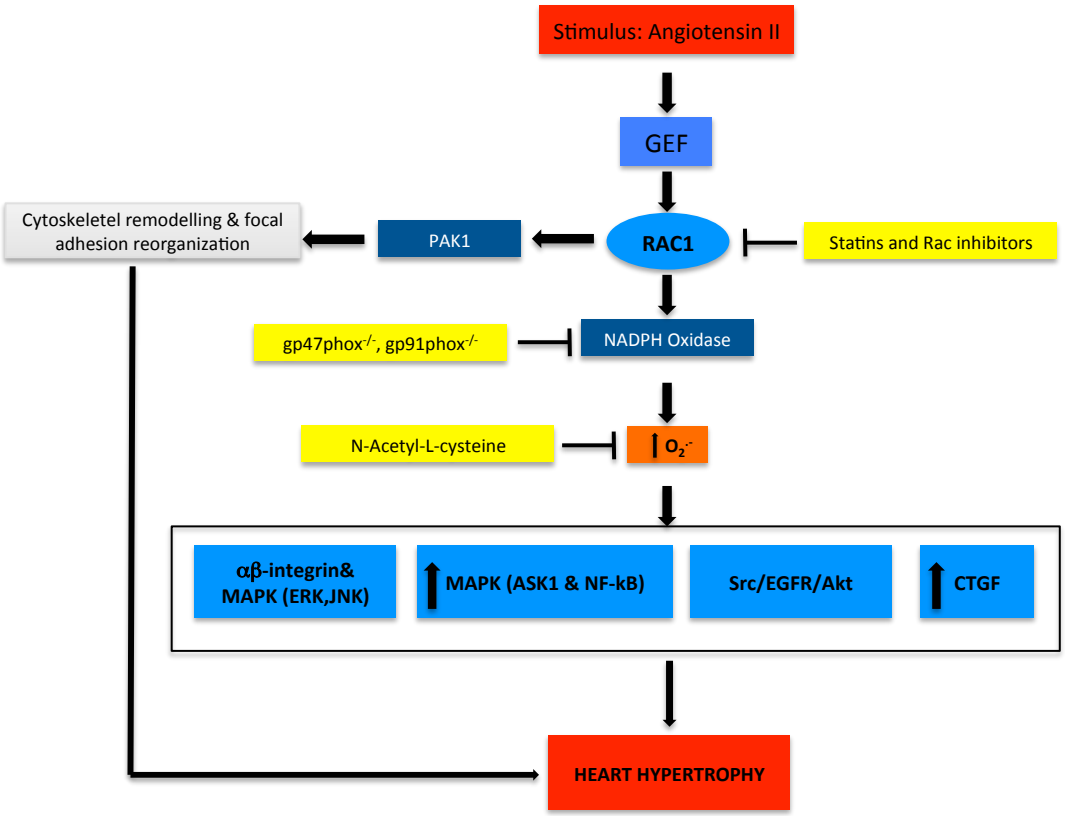

Figure3: Role of Rac/NADPH oxidase-derived oxidative stress in the development of cardiac hypertrophy. Rac1 inhibition with dominant negative Rac mutant (Rac-DN), Rac deletion ($Rac^{-/-}$) or statin, inhibition of NADPH oxidase with deletion of gp47phox (gp47phox-/-) or gp91phox (gp91phox-/-), or antioxidant such as N-acetyl-L-cysteine, could reverse these effects. Ang-II, angiotensin II; GEF, guanine nucleotide exchange factor; PAK1, p21-activated kinase 1; TGFβ, transforming growth factor-β; CTGF, connective tissue growth factor; EGFR, epidermal growth factor; MAPK, mitogen-activated protein kinase; ASK1, apoptosis signal-regulating kinase; NF-κB, nuclear factor-κB; ERK, extracellular signal-regulated kinase; JNK, c-Jun N-terminal kinase.

Although PAK binding has been used to document increased Rac1 activation, this effector seems to be dispensable for the Rac1-induced cardiomyocyte hypertrophy. In fact, PAK binding to Rac1 is not required to induce the transformation and lamellipodium formation, and activation of JNK, p38–

MAPK, and serum response factor; nevertheless, myocytes contractility is influenced by PAK[91].

Several profibrotic stimuli, including mechanical stretch, ischemia/reperfusion injury, phenylephrine, and angiotensin II, have been shown to promote the formation of ROS and Rac1 activity. For instance, the overexpression of N17Rac1 abrogates the mechanical stretch-induced intracellular ROS generation in cardiomyocytes. The same dominant-negative mutant of Rac1 inhibits the angiotensinII stimulation of ROS production in isolated cardiomyocytes. Subsequent studies have then established a link between Rac1, ROS production, and nuclear factor-kB (NF-kB) activity in the cardiomyocytes hypertrophy.

In vivo evidence

To explore the direct involvement of Rac1 in cardiovascular disorders, both cardiac specific transgenic and knock-out mice have been generated. Mice overexpressing the constitutively active form of Rac1 clearly evidence a dramatic cardiomyopathy phenotype. While hearts from non-transgenic mice show a progressive increase of size consistent with rapid postnatal growth, those from transgenic mice are enlarged with severely dilated chambers and thin ventricular walls. Atria are also increased in size although at lower extent. This phenotype was hypothesized to be the results of a deregulation of signaling by Rac1 and PAK, followed by loss of systolic function, and lethal dilated cardiomyopathy. Indeed, the absence of overt myofibril disruption

cardiomyocytes of transgenic mice suggests that heart failure is not caused by loss of myofibril organization. Differently from the dilated hearts observed in young mice expressing the constitutively active form of Rac1 that died spontaneously within 3 weeks after birth, hypertrophy becomes the dominant phenotype in juvenile mice associated with an increase of heart/body weight ratio, thickening of ventricular walls and loss of ventricular chamber area.

A subsequent study was performed by generating the cardiac specific Rac1 knockout mice; these mice were subjected to a hypertensive stress by infusing angiotensin II. Despite similar increases in systolic blood pressure, mice not expressing Rac1 in the myocardium, do not develop cardiac hypertrophy and show a significant reduction in end-diastolic myocardial wall thickness and left ventricular mass. These effects were associated to a smaller induction of cardiac fetal gene expression such as ANF, BNP, α-skeletal actin, and myosin light chain 2 ventricular isoform. The protective effect of the absence of Rac1 in the heart was associated with the inhibition of NADPH oxidase-dependent generation of $O_2^{\cdot-}$ and NF-κB transcriptional activity. Consistent with these findings ZmRacD transgenic mice, that express a constitutively active form of Rac1, spontaneously develop a distinct cardiac phenotype manifested by cardiac hypertrophy, relative ventricular chamber dilation, and moderate systolic dysfunction[92]. These mice are also more susceptible to post-ischemic injury and develop significantly larger myocardial infarcted area.

Interestingly, the gene deletion of the small GTPase protein Cdc42, which belongs to the same family of Rac1 and shares similar GEFs, makes the mice

more susceptible to develop cardiac hypertrophy, following pressure overload. This function for Cdc42 is unique among the Rho GTPase, as Rac1, Ras, and RhoA have all been shown to facilitate cardiac hypertrophy or myopathy in genetically modified mice, and indicates the importance to develop selective Rac1 inhibitors in order to have a potential cardioprotective effect.

Taken together the effect of Rac1 on cardiac hypertrophy has been demonstrated by both *in vitro* and *in vivo* experimental conditions either by regulating actin cytoskeletal assembly and sarcomeric organization or the oxidative stress by assembling the NADPH oxidase.

Clinical evidences

In patients with chronic heart failure, increased oxidative stress is associated with reduced left ventricular (LV) function and correlates with the severity of the disease[93,94]. Many animal studies suggests that in cardiomyocytes, NADPH oxidase may be a relevant source of ROS in cardiac hypertrophy and failure[95,96].

Rac1 must be prenilated for its translocation in membrane and its subsequent activation with exchange of GDP for GTP at its regulatory domain its a critical process in the activation of NADPH oxidase, moreover the activation of Rac1-GTPase mediates cellular hypertrophy of cardiac myocytes in experimental systems[97,98].

The prenilation step is inhibited by statins reducing translocation of Rac1 to the cell membrane, therefore the inhibition of Rac1 by statins decreases

NADPH oxidase–related ROS production in vascular smooth muscle cells and cardiac myocytes and reduces cardiac hypertrophy in both in vitro and animal experiments[99–101] these therapeuthic effects are correlated to the so called pleyotropic effects of statins.

In patients affected by chronic heart failure which is associated a reduced left ventricular function was observed an increased oxidative stress and correlates with severity of the disease. Although the source of ROS in chronic heart failure remains to be elucidated, emerging evidences suggest that Rac1-mediated NADPH oxidase activation plays a prominent role. The administration of statins, has also shown to significantly inhibits myocardial Rac1-GTPase activity with a potential beneficial effects for patients with chronic heart failure[102]. Statins also improves redox state in saphenous vein grafts in patients undergoing to coronary artery bypass grafting by inhibiting Rac1-mediated activation of NADPH oxidase, further confirming the central role of Rac1 in cardiac heart failure and hypertrophy.

In human failing myocardium, upregulation of Rac1 and p47*phox* membrane protein expression as well as increased Rac1-GTPase activity may resemble the underlying mechanisms for increased oxidase activity.

However, especially in human myocardium, the precise mechanisms of this link require additional investigations. Because activation of Rac1-GTPase may contribute to the development of heart failure, so from the threatment with statin is attempted to inhibit Rac1 in human myocardium.

To address these issues, patients awaiting elective coronary bypass surgery

were prospectively treated with pravastatin, atorvastatin, or without statin. After 4 weeks of statin treatment, activity as well as expression of Rac1 in right atrial myocardium was significantly reduced compared with untreated controls.

Therefore the increased Rac1-GTPase activity is associated with enhanced NADPH oxidase–related ROS production. Furthermore, oral treatment with both a lipophilic and a hydrophilic statin inhibits Rac1-GTPase activity and reduces Ang II–induced NADPH oxidase activity in atrial myocardium. However a prospective, randomized clinical trial is necessary to address whether statin treatment is beneficial in patients with chronic heart failure.

Further confirm that Rac is strongly related to cardiovascular disease in human, in patients with end-stage heart failure with dilated cardiomyopathy and ischemic cardiomiopathy were observed that Rac1-GTPase activity was upregulated 3-fold compared with non failured myocardium[102].

The pathogenesis of atherosclerosis

Atherosclerosis is a multifactorial disease that involves the vascular district causing the occlusions of large conduit arteries such as aorta and iliac and medium caliber as coronary, carotid and femoral arteries.

This disease is responsible for the onset of pathological vascular events such as myocardial infarction and stroke which are the main cause of mortality and morbidity in the United States, Europe and Japan[103].

Arteries are constituited by three different layers: the tunica intima, media and

adventitia .The tunica intima is the innermost layer of the vessel wall and is constituted by a thin internal layer of endothelial cells that separates the lumen to artery wall. The cells belonging to this layer express proteins such as nitric oxide synthase and thrombomodulin that in normal conditions confer anti-adhesive and antithrombotic properties to the vessel wall. The tunica media is composed of smooth muscle cells and from the extracellular matrix. Tunica intima, unlike the tunica media, generally does not vary with aging. The tunica adventitia is separated from the media by the external elastic lamina and is composed mainly of fibroblasts, collagen and glycosaminoglycans .

The endothelial dysfunction leads to an injury and a compensatory response that alters the normal homeostatic properties of the endothelium and involve an increase in the adhesiveness of leukocytes and platelets. Cellular damage also induces the endothelium to have procoagulant properties and form vasoactive molecules, cytokines and growth factors. These factors make the injury a favorable environment for the formation of thrombosis.

The inflammatory response also stimulates the migration and proliferation of SMC that migrate from the tunica media to the intima. If these responses continue undisturbed can thicken the artery wall which will compensate with a gradual expansion to keep the diameter of the lumen unaltered, this phenomenon is called "Glagov" or remodeling[104]. The continuous inflammatory state, moreover, involves an increase in the number of macrophages and lymphocytes that arrive from the bloodstream into the inflamed area and multiply within the lesion. This cycle of accumulation of

mononuclear cells, migration and proliferation of smooth muscle cells and the formation of fibrous tissue involves the successive enlargement and remodeling of the lesion. These events lead to the formation of a fibrous cap that covers the lipid core and necrotic tissue[103].

Plaque rupture is a very dangerous event that can lead to myocardial infarction and cerebral stroke. To determine the rupture of the plaque there are many internal factors related to the structural characteristics of the lesion but also external factors. Histological studies of human atherosclerotic lesions have allowed to observe that the accumulation of macrophages and the presence of fibrous caps purposes, containing few smooth muscle cells, are characteristics of plaques "unstable" or more susceptible to rupture. The size and texture of the atheromatous core vary considerably, but both characteristic are important in order to evaluate the stability of the plaque: plaques containing a soft core are more subject to rupture and to originate acute ischemic pathologies.

The lipids, as cholesterol esters, tend to soften the plaque, while cholesterol crystals have an opposite effect[105,106]. This theory is supported by observations made as a result of lipid-lowering therapies in humans that lead to a general reduction of the content of cholesterol esters and to a relative increase of deposit of cholesterol crystals within the atheromatous core, factors that determine a greater plaque stability[107].

In the core of the plaque there is highly thrombogenic material and, for this reason, the fibrous caps became fundamental to separate the core from vessel

lumen avoiding that these two environments are in contact. The fibrous caps can vary greatly in thickness, number of cells, resistance, quantity and constitution of the matrix, however, a concept common to all is that the thinning of the cap and the reduction of collagen content and smooth muscle cells lead to increased susceptibility to break[108].

Among the various components, collagen plays a key role in order to confer resistance to the tissues and thus also to the fibrous cap, in fact, experimental evidences suggest that plaques containing lower concentrations of collagen are more prone to rupture compared to those rich in this protein[109].

Role of Rac1 in atherosclerosis

Role in vascular smooth muscle cell proliferation, migration, and differentiation

In advanced atherosclerotic lesions smooth muscle cells accumulation in the intima results from cell proliferation and directed migration of smooth muscle cells from the media[110,111]. These processes are regulated by various factors that are produced locally at the sites of vascular lesion by macrophages, T-lymphocytes, platelets, endothelial cells and smooth muscle cells (Figure4). Among these, platelet derived growth factor (PDGF) and tumor necrosis factor-α (TNF-α) are the best characterized[112].

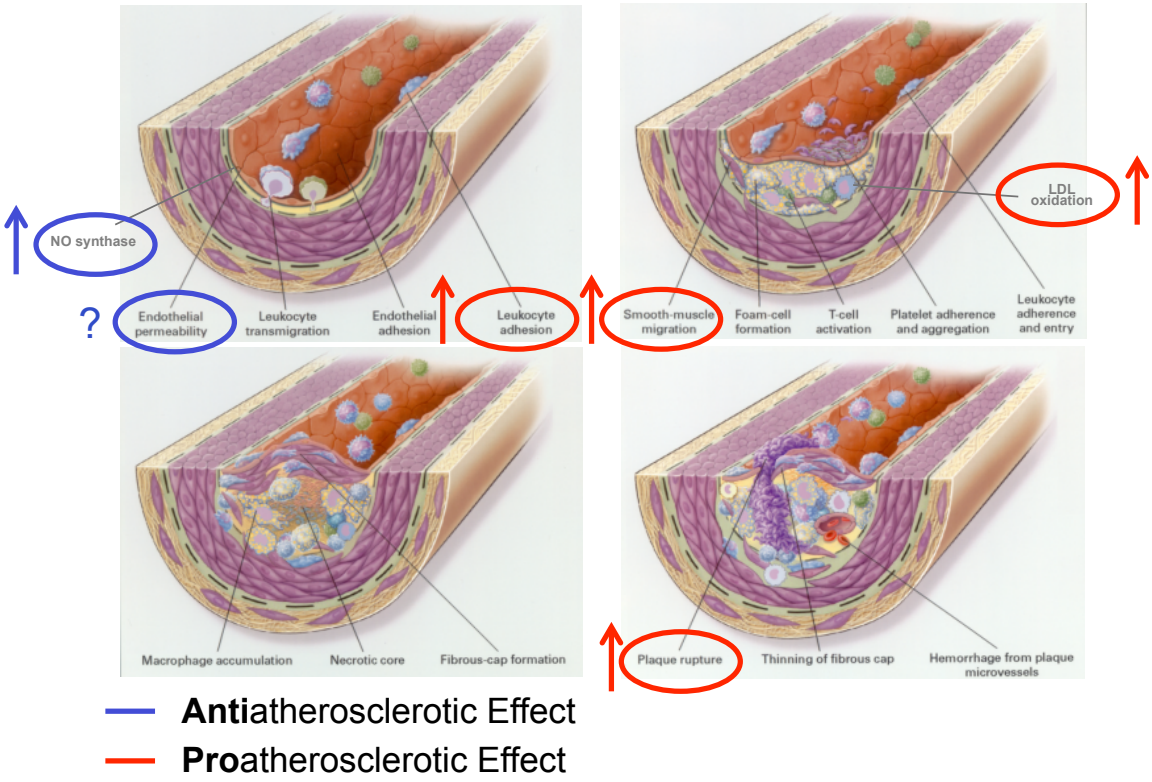

Figure4. Role of Rac1 in atherosclerosis.

The requirement of Rac1 for smooth muscle cell migration in response to PDGF was first demonstrated by expressing the dominant negative form of Rac1 (N17Rac1)[113] . The site specific Rac1 activation in response to PDGF is regulated by RhoB which coordinates the endosomal trafficking of Rac1[114]. This rapid remodeling of the plasma membrane and underlying actin cytoskeleton is drastically affected in smooth muscle cells depleted of the focal adhesion kinase (FAK)[115]. Indeed, PDGF treated FAK$^{-/-}$ smooth muscle cells remain unpolarized without forming a distinctive leading edge. Importantly, the absence of FAK does not alter the total Rac1 activity but affects the restricted enrichment of Rac1 at the leading edge. More recently, it has been identified the role of the Ahnak protein as a scaffold module that promotes the

interaction of Erk -PAK -β-PIX protein complex with Rac. The Ahnak protein is indeed required for PDGF- demonstrated that, in response to a chemotactic agent, localized Rac1 activity and actin cytoskeleton assembly at the leading edge coordinate the smooth muscle cell migration.

Smooth muscle cell migration in response to PDGF is also dependent by the activity of the NADPH oxidase which generates the ROS and the phosphorylation on Thr423 of the Rac1 effector PAK1[116]. In vitro stimulation of smooth muscle cells with thrombin upregulates the expression levels of Nox1, an inducible isoform of NADPH oxidase[117], which modulates [Ca2+]i levels partially via influx of extracellular Ca2+. Small interfering RNA directed against Nox1 blocks the basic fibroblast growth factor (bFGF)-induced ROS generation as well as cell migration[118].

TNF-α is another potent proinflammatory cytokine, produced by macrophages and and lymphocytes in atherosclerotic lesions and in the intima of arteries after injury that promotes the accumulation of smooth muscle cells[119–121]. In vitro experiments, conducted in human coronary artery smooth muscle cells, demonstrated that p38-MAPK/CREB/Rac1 pathway plays a critical role in TNF-α- induced smooth muscle cell migration[122].

The activity of Rac1 influences also the transition of smooth muscle cells from the quiescent state to a synthetically active and proliferative phenotype in the vessel wall media. The expression of Rac1 is enhanced under vessel cyclic strain and positively regulates h1-calponin, a marker of contractile phenotype[123]. With this regard, type I fibrillar collagen, surrounding smooth

muscle cells in the media, regulates cell behavior and Rac1-dependent matrix metalloproteinase 1 expression[124].

Rac1 is then required for smooth muscle cell proliferation by inducing Skp2, the F-box component of the SCFSkp2 ubiquitin-ligase that promotes ubiquitin-mediated proteosomal degradation of $p27^{Kip1}$ [125], and by upregulating the cyclin D1 mRNA 70 (Table 2). Taken together, Rac1 is a key signaling molecule activated by different cardiovascular agonists and involved in SMC migration proliferation and differentiation processes potentially associated with atherosclerotic plaque development.

Regulation of endothelial permeability and leukocyte diapedesis in the vascular wall

The movement of leukocytes from the blood into the arterial wall plays a key role in the inflammatory response associated to atherosclerosis[126] and the activation of integrin receptors on leukocytes, in response to adhesive and chemoattractant agonists, mediates their arrest on the endothelium monolayer. Spatially and temporally restricted Rac1 activation to the leading edge is required during α4β1-integrin dependent leukocyte migration on both the vascular ligand VCAM1 (vascular cell adhesion molecule 1) and on the extracellular matrix 10 protein fibronectin[127]. Furthermore the ligation of α4β1-integrin directly regulates Rac1 activation and leukocyte migration[128]. This event is considered to be just one of those that contributes to leukocyte transendothelial migration. Certainly other cues that drive migration, such as

chemoattractants and signals generated by mechanical force on the cell (such as shear flow), will come into play to regulate Rac1 activation and cell migration. The combined input of these cues will ultimately determine how and where leukocytes migrate. Moreover, the fact that both active and dominant negative form of Rac1 inhibit macrophage migration suggests the requirement for a balanced and coordinated regulation of Rac1 for a proper leukocyte migration[129,130]. Rac1-dependent NF-kB activation is also required for the subsequent flow-induced surface expression of ICAM-1[131], which is involved in the recruitment of leukocytes into the atherosclerotic plaque. These evidences put Rac1 in a central role into the leukocyte diapedesis and inflammation in response to vascular injury.

Rac1 becomes activated within 5 to 30 minutes after shear stress stimulation and is required for respreading and alignment of endothelial cells in the direction of flow [132]. The Rac1 effector PAK is directly involved in the regulation of endothelial permeability and its inhibition, in vivo, reduces vascular permeability in atherosclerosis-prone regions[133,134]. The effect of PAK on endothelial permeability is also associated with increase NF-κB activation and probably involves both ROS and actin cytoskeleton reorganization[134,135]. In contrast with this observation, activated Rac1 also promotes the breakdown of cell-cell junctions and endothelial permeability[136]. The dual role of Rac1 is probably dependent by the effector pathways that is recruited under different stimuli.

Elevated permeability of the endothelium is believed to allow entry of

lipoproteins into the vessel wall, which become oxidized and propagate endothelial dysfunction and foam cell formation. The endothelial barrier property is tightly regulated whereby IQGAP activation has been suggested to stabilize the adherens junctions[136], whereas PAK activation is linked to increased endothelial cell permeability[137]. Thus, conditions that favor interaction of Rac1 with PAK would lead to junctional disruption, whereas those that favor IQGAP would lead to junctional stabilization. The protective role of Rac1 on the endothelial function has also been associated with the regulation of eNOS activity in vascular permeability is still debated and will need to be investigated in in vivo experimental models.

In vivo evidence on atherosclerosis

The majority of currently reported data on the role of Rac1 in atherogenesis are related to its functional role in the NADPH oxidase activity and oxidative stress. Different knock-out mice have been generated with the aim to alter the oxidative balance or the function of redox- sensitive proteins and transcription factors[138,139,140,141,142,109-113]. Smooth muscle cells isolated from mice lacking the p47phox subunit of the NADPH oxidase show a lower superoxide production and a reduced proliferative index in response to growth factors compared to wild type mice[141]. ApoE$^{-/-}$ mice crossed with p47phox-/- mice develop smaller atherosclerotic lesions compared to apoE$^{-/-}$ single knock out, regardless the type of diet utilized[141]. In response to wire injury, gp91phox-/- mice develop smaller lesions in the femoral artery associated with less pronounced

hyperproliferative response compared to wild type mice[142]. This effect seems to be the results of a lower proliferative capacity of smooth muscle cells gp91phox-/-[142]. A similar defect in cell proliferation, determining a lower neointima formation in response to vascular injury associated to lower activation state of Rac1, was observed in smooth muscle cells isolated from CHF1/Hey2-/- mice[143]. The CHF1/Hey2 is a cardiovascular-restricted, hairy-related bHLH transcription factor, whose endothelial Rac1 haploinsufficient mice[144].Thus, the final outcome of Rac1 inhibition or deletion leads to cardiomyopathy in adult mice[145]. The absence of CHF1/Hey2 does not affect the expression of PDGF or EGF receptors, activation of the MAP kinases ERK1/2, p38, or activation of the survival kinase AKT but decreases Rac1 activity and the Rac-GEF, Sos1, expression[138].

The Rac1-dependent generation of the ROS also mediates the effect of Ref-1 on PDGF-induced smooth muscle cell migration[140]. Ref-1 is an apurinic/apyrimidinic endonuclease/redox factor-1 involved in the base excision repair pathways of DNA subjected to oxidative damage and, in addition, promotes a variety of redox mediated events. In smooth muscle cells, Ref-1 appears to be downstream of Rac1 in the chemotactic response to PDGF, and its deletion determines a lower neointima formation in response to balloon injury[140]. Another factor linked to the oxidative response is the transcription factor nuclear factor erythroid 2-related factor 2 (Nrf2). Many studies have reported a pathophysiological role of Nrf2 in protecting cells from oxidative stress and Nrf2 null mice show enhanced neointima hyperplasia and

higher basal and PDGF- stimulated Rac1 activity in smooth muscle cells[139]. Finally, the haploinsufficient mice for kalirin-9, a protein abundantly expressed in smooth muscle cells containing two GEF domains for Rac1 and RhoA, develop 60% less neointima than WT mice. This effect was demonstrated to be associated to lower Rac1 activation and to be smooth muscle cell specific[146]

Selective Rac inhibitors and their mechanism of action

Before the development of new selective inhibitors, the pharmacological blockade of the small GTPases has been described with the use of the HMG-CoA reductase inhibitors, statins[147], and the prenyl transferase inhibitors [148,149]. Both type of agents inhibit the isoprenylation processes of different intracellular proteins and, thus, their activity in a nonselective manner. This nonlipid-related effects of statins are thought to contribute to their protective action on cardiovascular events, thus supporting the development of selective inhibitors of the small GTPase proteins[102,150,151]. In *in vitro* and *ex vivo* analyses, indeed, have demonstrated that statins inhibit the isoprenylation and function of both RhoA and Rac1[124,152]. Moreover, a novel pleiotropic mechanism of statins has also been described that does not involve the isoprenylation process but the increase nuclear translocation and degradation of Rac1. These evidences supported the interest in the development of new selective Rac1 inhibitors and to investigate their effect in cardiovascular diseases (Table1).

Compound	*Chemical structure*	*Mechanism of action*	*Potency (cultured cells)*
NSC23766 [99]	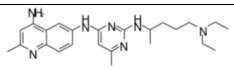	Inhibition GEF-Rac1 interaction (selective for Tiam1 and Trio)	50 μM
ITX3 [103]	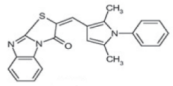	Inhibition GEF-Rac1 interaction (selective for Trio)	100 μM
EHop-016 [105]	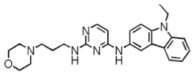	Inhibition GEF-Rac1 interaction (selective for Vav2)	1.1 μM
EHT 1864 [106]	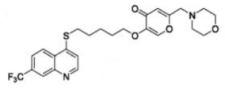	inhibition of Rac1 nucleotide binding (possible allosteric mechanism)	≈5 μM
Compound **5** [100]	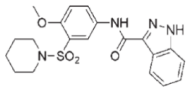	Inhibition GEF-Rac1 interaction (Tiam1)	24.1 μM
Compound **4** [102]	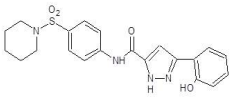	Inhibition GEF-Rac1 interaction (Tiam1, Trio and Vav2)	8.7 μM
Phox-I1 [107]	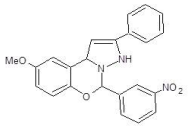	Inhibition effector-Rac1 interaction (p67*phox*)	≈10 μM
8-OHdG [108]	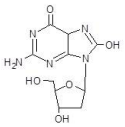	Inhibition of Rac1-dependent NADPH oxidase activity	≈156 μM

Table1: Chemical structrure and molecular mechanisms of Rac inhibitors.

Rac1–GEF interaction inhibitors

The determination of the crystal structure of the DH and PH domains of the T-lymphoma invasion and metastasis factor 1 (Tiam1) GEF in complex with Rac1 has provided detailed information on the mechanism and the specific sites of GEF-Rac1 interaction[153]. In particular, Trp[56] of Rac1 is a critical site for the discrimination of a subset of GEF, including Tiam1 and Trio[154]. These studies have allowed the identification of a polypeptide derived from the b3 region of Rac1 including Trp[56] that serves as a specific inhibitor for Rac1 interaction with the GEFs. Further implementation of this study led to the identification, by a structure-based virtual screening approach, of the first selective inhibitor

of Rac1, compound NSC23766[155]. This small molecule fits into the surface groove of Rac1 involved in the binding with GEFs, thus interfering with the Tiam1–Rac1 interaction. The selective action of NSC23766 was demonstrated to be restricted to the 2 GEFs, Trio and Tiam1, without interfering with the GEF for the RhoA, the PDZ-Rho, the GAP Rac1- Bcr, and the effector PAK1[155].

In cell-based experiments, NSC23766, at concentration of 50–100 μM, reduced Trio- or Tiam1-mediated cell growth and transformation without a significant effect on Vav (Rho/ Rac/Cdc42 GEF), Lbc (Rho GEF), and intersectin (Cdc-42 GEF) stimulation[155].

A more specific inhibitory action was then observed for the compound ITX3 that interferes with Trio without affecting the activation of Rac1 by both Tiam1 and Vav2[156]. This compound was derived from a previous screening of 3500 chemical entities using a GEF activity assay[156,157]. In a cell-based pharmacological test, the compound ITX3 inhibited the formation of TrioN-dependent cell structures in a dose-dependent manner, with an IC_{50} value of approximately 100 μM[156].

The most potent Rac1 inhibitor so far identified is the compound EHop-016, with an IC_{50} value of 1.1 μM, approximately 50-fold lower than that of NSC23766. Ehop-016 was discovered by optimizing the chemical structure of NSC23766[158]; however, it does not show a very selective activity on Rac1 because it also acts on Cdc42. Different from NSC23766, Ehop-016 effectively inhibits the association of active Vav2 with the Rac1[158].

Allosteric inhibitors of nucleotide binding to Rac1

EHT 1864 is another very interesting compound that selectively reduces the intracellular levels of Rac1–GTP, with an IC_{50} value of 5 μM. The biochemical analyses performed with recombinant Rac1 found that EHT 1864 possesses high-affinity binding to Rac1, and the related Rac1b, Rac2, and Rac3 isoforms, and this association promoted the loss of bound nucleotide, placing Rac in an inert and inactive state, preventing its engagement with downstream effectors. This effect seems to be the result of an inhibitory allosteric mechanism[159].

Antagonists of Rac1-mediated NADPH oxidase activity

Phox-I1 is the most recent type of Rac1 inhibitor that has been described. Phox-I1 targets the interactive site of p67phox with Rac1 GTPase with a submicromolar affinity and very efficiently inhibits the ROS production in neutro- phils at 20 μM concentration[160]. As expected, a similar effect was observed with compound NSC23766 at 100 μM[160], but different from Phox-I1, NSC23766 also abrogated the phos-phorylated PAK levels. Thus, different from the inhibitors of GEF–Rac interaction, the compound Phox-I1 acts selectively on the Rac1-dependnet NADPH oxidase activity.

The 8-hydroxy-2-deoxyguanosine (8-OHdG) represents, today, the only Rac1 inhibitor that has been tested in an in vivo model for atherosclerosis[161]. 8-OHdG act by inhibiting the ROS production in macrophages and neutrophils by blocking the NADPH oxidase activity[162,163,164], and a similar action has been shown on Ang-II and PDGF-mediated oxidative stress in SMCs. The effect of 8-OHdG (30 mg/kg21/d21) was tested in $apoE^{-/-}$ mice after a partial ligation of

the left common carotid artery[165]. After 2 weeks of treatment, the lesion area was significantly reduced in treated animals compared with vehicle (approximately 60%) that led to prevention of vessel lumen occlusion. This protective effect was associated with reduced ROS levels in the arterial wall and macrophage accumulation. In vitro studies also documented that 8-OHdG inhibits SMC proliferation and cell adhesion molecules expression, in response to PDGF.

Small animals models of heart hypertrophy

The study of heart failure requires viable animal models whereby chronic changes in myocardial structure and function can evolve and the progression of heart failure and left ventricular (LV) dysfunction can be quantified (Table2).

SPECIES	MODEL	HEART FAILURE STIMULUS	ADVANTAGES	DRAWBACKS
RAT	Left coronary ligation	MI	• Availability of multiple modalities to assess cardiovascular function • Surgical techniques easier than in mice • Greater quantity of myocardial tissue for postmortem analyses • Lower cost than large animal models allows for greater "N"	1. Lack of transgenic or knockout strains 2. Expense of equipment for cardiovascular physiology assessment 3. Favorable results not always reproduced in clinical studies
RAT	Ascending aortic constriction	Gradual onset pressure overload	• Gradual onset hypertension Also see above for rat MI model	1. See above for rat MI model
RAT	Dahl salt-sensitive rat	Chronic pressure overload	• No surgery required for heart failure stimulus • Gradual onset hypertension induced by a high-salt diet • Heart failure develops gradually, may be more clinically relevant • Also see above for rat MI model	1. High cost of maintaining colonies for an extended period as heart failure develops (6–12 months or more) 2. Also see above for rat MI model
RAT	Spontaneously hypertensive heart failure–prone rat	Chronic pressure overload	• No surgery required for heart failure stimulus • Hypertension is more gradual onset. Heart failure, therefore, occurs in later stages and thus may be more clinically • relevant Also see above for rat MI model	1. High cost of maintaining colonies for an extended period (6–12 months) 2. Also see above for rat MI model
MOUSE	Left coronary ligation	MI	• Lower cost than rats Ability to assess cardiovascular • physiology using multiple • modalities Wide availability of transgenic or • knockout strains of interest including specific cell type or inducible transgene expression	1. Significant expertise and expense required for mouse surgery or assessment of cardiovascular physiology or both 2. Limited myocardial tissue limits the no. of biochemical analyses that can be performed 1. See above for mouse MI model 2. Vast overexpression of biologically inert proteins may nonspecifically cause dilated cardiomyopathy
MOUSE	Transverse aortic constriction	Acute and pressure overload	• See for mouse MI model Potent stimulus for hypertrophy • that develops rapidly thus reducing follow-up time (1–2 weeks)	1. Hypertension is acute not gradual in onset and thus lacks direct clinical relevance 2. See row above for mouse MI model
MOUSE	Muscle lim protein knockout	Dilated cardiomyopathy	• No surgery required for heart failure stimulus • See above for mouse MI model	1. See above for mouse MI model
MOUSE	Cardiomyocyte- specific overexpression of TNF-α	Dilated cardiomyopathy	• No surgery required for heart failure stimulus • See above for mouse MI model	1. See above for mouse MI model 2. Vast overexpression of biologically inert proteins may nonspecifically cause dilated cardiomyopathy
MOUSE	Administration of Ang II Through osmotic pump (Alzet)	Heart hypertrophy	• Continuous delivery ensures constant compound levels in plasma or tissues for maximized therapeutic efficacy and reduced adverse effects. • The implantion of this pump not require any particular expertise. • The ability to implant these pumps under the skin with or without catheter can minimize the chance of animal interference and infection.	1. High variability

Table2. Different animal models for hart hypertrophy and heart failure

Heart failure in rats

The rat heart failure models are charecterized of numerous potential advantages inherent in a small animal model. Housing and maintenance costs are much lower than for large animals, these allow to increase the number of animals included in a given study to improve the statistical power. Moreover, more recent technological advances in echocardiography, MRI, and micromanometer conductance catheters have greatly streamlined the assessment of cardiac function in rodents, removing a significant barrier to their use in heart failure research. The development of suitable expertise to perform open-chest surgical procedures and invasive hemodynamic assessments in rats is far easier compared with that required for mice. Additionally, investigators are able to perform a greater number of postmortem histological or molecular biological analyses given the approximately 10-fold greater myocardial mass of rats compared with mice.

Rat models of myocardial injury

Originally myocardial infarctions in rats were induced by the sequential administration of subcutaneous isoproterenol causing diffuse myocardial necrosis[166]. Subsequently another techniques was developed by using an electrocautery applied to the epicardial surface to induce small, focal infarctions[167].

Finally, Pfeffer et al[168] developed the rat coronary ligation model that became the most widely used heart failure and MI model in the decades. Infact, this

model is usefull to explore the relationship between infarct size and LV chamber dilatation and function. They observed a proportional increase in LV volume as a function of infarct size that was a highly original and novel finding[169], at which time, the notion that vasodilators may "unload" and therefore benefit failing hearts was gaining momentum.

Angiotensin-converting enzyme inhibitor, captopril, therapy reduced LV chamber dilation, improved LV systolic function, and increased survival in rats with moderate or large myocardial infarctions[170,171].

This innovative myocardial infarction model in rats led to clinical trials testing the utility of the angiotensin-converting enzyme inhibitor, captopril, in post-miocardial infarction patients with reduced LV function. Therefore at the end of a large multicenter clinical trials captopril decreased all-cause mortality by 19% with a 22% reduction in heart failure hospitalizations after a mean follow-up period of 42 months[172]. The reductions in mortality and morbidity were associated with less LV dilation or remodeling during the first year of therapy[173], this is a clear example of the utility of small-animal models to explore new and potentially important therapies for heart failure.

Miocardial infarction model was also essential in establishing the beneficial effects of angiotensin II type 1 receptor antagonists on LV structure and function following miocardial infarction[174,175]. However, the case for endothelin receptor antagonists illustrates that results in this model are not necessarily mirrored in clinical heart failure trials.

Rat pressure overload models

Ascending aortic banding

The ascending aortic banding is one of the more widely used surgical models to induce pressure overload in rats. During the rats growth hypertension develops gradually, during which aortic outflow is increasingly impeded. Lorell and colleagues[176] developed this model and showed that 8 weeks postbanding, rats exhibit maintenance of LV chamber size with clear evidence of LV hypertrophy, consistent with "compensated hypertrophy" though Doppler echocardiography at this stage shows evidence of increased left atrial pressure. 18 weeks, overt signs of heart failure become evident (ie, tachypnea, edema, pleural effusions, and ascites) that are associated with LV dilation and systolic dysfunction.

The advantages and disadvantages in this model are similar to those noted for the rat miocardial infarction model with the added benefit that the stimulus for heart failure (pressure overload) is gradual in onset as is the progression from compensated hypertrophy to decompensated heart failure, therefore making this model potentially more clinically relevant to heart failure progression in humans. Hajjar and colleagues[177,178] have used this model extensively to explore the utility of adenoviral- mediated gene therapy to restore levels of the calcium handling protein, Serca2A, whose expression is diminished in failing hearts.

Once optimized the tecnique and achieved the adequate myocardial expression of Serca2A construct wich resulted in a clear improvements in LV systolic

function, remodeling, and survival. Following preclinical studies in larger animal models, this novel gene therapy approach has now entered the clinical arena as a phase 1 clinical trial[179].

Genetic models of hypertension and heart failure in rats

In the Dahl salt-sensitive rat, hypertension and heart failure develop gradually in rats placed on a high-salt diet. LV hypertrophy without chamber dilatation develops within 4 to 6 weeks of a high-salt diet followed by a decompensated phase of heart failure and LV dilation at approximately 15 to 20 weeks[180]. Another commonly used rat model of spontaneously hypertensive heart failure- prone has been developed by McCune et al[181]. Moreover Heyen et al[182] demonstrated that progressive LV hypertrophy with normal ejection fraction develops between 4 and 9 months of age; by 12 months, LV dilation and decreased LV systolic function occurs in tandem with a marked rise in circulating cytokine levels including tumor necrosis factor TNF-α and interleukin-6.

These genetic models of pressure overload and heart failure offer several advantages. Infact in these models is not required any surgical expertise and moreover the gradual onset of hypertension with aging has more direct clinical relevance, with both models being characterized by time-dependent, progressive LV hypertrophy in the early stages followed by the development of heart failure and LV dysfunction in later stages.

Genetic models resulted also less expensive for the cost associated with maintaining colonies for an extended period of time (6 to 12 months) to allow

emergence of the heart failure phenotype.

Heart failure models in mice

The greatest benefit in using mouse models is the availability of a great number of relevant transgenic and knockout strains. The advent of cell type-specific, inducible knockout or transgenic strategies has made the mouse an invaluable tool to study the pathogenesis of heart failure and to identify novel therapeutic targets with lower housing costs compared with rats. In addiction cardiac physiological assessments have been facilitated greatly by newer technologies such as ultrahigh resolution ultrasound[183] and micromanometer conductance technology for pressure volume loop analyses[184,185]. However, these new methods are very expensive and pose significant technical challenges to laboratories without an appropriate expertise. Whereas the rat models listed above have been used extensively to explore the potential for novel pharmacological or molecular agents for the treatment of heart failure, mouse models are best used as "proof of principle" to identify important gene or protein targets that pave the way for the development of new molecular or pharmacological therapies.

Mouse models of myocardial injury

The denvelopment of transgenic and knockout mouse models determined new important approaches to study disease and therefore the development of surgically induced mouse models of heart failure became necessary. 30 years

ago was described a first mouse model of coronary ligation.

Recently Michael et al[186]. Estabilished a first mouse model of ischemia-reperfusion injury. In this model they identified that mouse left coronary anatomy is highly variable. Porter et al. developed a model of permanent coronary ligation in mice and others effort to gain further insight into pathophysiology of post-miocardial infarction cardiac remodeling[187,188].

Mouse models of heart failure can be used to identify potentially important and novel targets for pharmacological or molecular therapy.

Many studies with overexpression or KO of proteins (ie, CaMKII) exemplify how mouse models can unveil the physiological relevance of a given protein using complementary overexpression and molecular and pharmacological strategies.

Mouse pressure overload model of transverse aortic constriction

The transverse aortic constriction (TAC) model is the most widely used model; it was first described by Rockman et al.[189,190]. The greatest advantage of this model is the ability to quantify the pressure gradient across the aortic structure that allows stratification of LV hypertrophy. The sudden onset of hypertension achieved with TAC causes an approximately 50% increase in LV mass within 2 weeks, making this model an excellent choice to examine the utility of pharmacological or molecular interventions that may limit hypertrophy.

An important drawback of the TAC model is the variability in the LV

remodeling responses among different mouse strains: C57BL6 mice develop rapid LV dilation[191] after TAC that may not occur with other strains. Another important aspect is that the acute onset of severe hypertension characteristic of this model lacks direct clinical relevance.

Genetic models of dilated cardiomyopathy in mice

Numerous KO or transgenic mice have been developed that have implicated a given protein in the pathogenesis of heart failure and dilated cardiomyopathy. Arber et al[192] developed a model of dilated cardiomyopathy in which homozygous deletion of the gene encoding muscle lim protein caused myofiber disarray, LV hypertrophy, dilation, systolic dysfunction, and heart failure.

Muscle lim protein is an actin-based cytoskeletal protein that positively regulates myogenic differentiation. The authors hypothesized that its disruption may uncouple mechanical load from the induction of muscle-specific genes that maintain striated muscle function. Indeed, muscle lim protein knockout mice develop a cardiac phenotype resembling dilated cardiomyopathy characterized by the development of LV dysfunction, heart failure, and death. Muscle lim protein knockout mice have since served as a genetic model of heart failure that is used by many laboratories to explore molecular therapies that might "rescue" the heart failure and dilated cardiomyopathic phenotype.

Another example of dilated cardiomyopathy was the TNF-α overexpressing mice. In this model mice develop LV hypertrophy, dilatation, and profound

systolic dysfunction associated with heart failure and premature death[193].

Treating these mice with a soluble chimeric protein comprised of the TNF-α receptor bound to an IgG fragment neutralizes circulating TNF-α and improves indices of cardiac function in these mice[194,195].

Howerver the positive effects of soluble TNF receptor chimera viewed in mice models didn't offer no morbidity or mortality benefits to patients with heart failure and LV systolic dysfunction, illustrating that positive results in preclinical rodent studies do not necessarily translate to clinical benefits when applied to heterogeneous heart failure populations.

Mouse models of heart hypertrophy induced by Angiotensin II

A model of heart hypertrophy in mice was developed by a continuous infusion of angiotensin II by means of an osmotic pump leading to sustained increased of systolic blood pressure. This model causes an eccentric hypertrophy, with increasing left ventricle mass and cardiomyocyte cross-sectional areas and reduction of ejection fraction.

Ang II treatment increase the production of $O^{\cdot -}$ of 3.3 fold in cardiac tissues respect WT, this increasing is in accordance with the improvement of NADPH oxidase activity is incresed of 1.9 fold. Moreover in these mice there is an increase of cardiac fetal gene expression, in particular, ANF and BNP.

With this model Liao et al.[196] demontrated how NADPH oxidase plays a critical role in the development of cardiac hypertrophy in response to Ang II, in particular the small G protein Rac1 through interaction with gp91phox and the

cytosolic components of NADPH oxidase, p67phox and p47phox, plays an important role for its activation.

Therefore the treatment with AngII activates NADPH oxidase, increases O_2 production, induces cardiac fetal gene expression, and leads to increased LV mass. All of these effects of Ang II on the heart occurred with similar changes in blood pressure and were decreased or absent in mutant mice with decreased cardiac expression of Rac1.

This model appears to be suitable only in a subset of animal strains since some of them are resistant to angiotensin. Moreover, the morphological response and the alteration of heart function it was found to be quite variable among the same group of animals, probably due to the not consistent release of AngII by the osmotic pumps. However, the advantage of this model is that very closely mimics the pathological conditions of hypertensive patients with high RAS activation and does not require significant experimental expertees.

Purpose of the research

In the last decade, the small GTPase protein Rac has gained increasing attention for its role in cardiovascular diseases. Transgenic mice expressing a constitutively activated Rac1 mutant in the myocardium developed either a lethal cardiac dilated phenotype or a transient cardiac hypertrophy that resolved with age[197]. In line with this evidence, cardiomyocyte knock-out specific mice for Rac1 are resistant to cardiac hypertrophy induced by angiotensin infusion[198]. The role of Rac1 in cardiac function has been associated with its regulatory function on the NADPH activity and thus generation of reactive oxygen species[198]. Moreover, endothelial Rac1 haploinsufficient mice showed decreased expression and activity of eNOS, which correlated with the decrease in endothelium-dependent vasorelaxation and caused mild hypertension[199]. This evidence suggests a protective role of Rac1 in endothelial cells and more in general in vascular diseases. Various agonists and extracellular matrices appear to be required for a proper Rac1-mediated modulation of endothelial barrier properties, through the involvement of reactive oxygen species and the actin cytoskeleton[200–202]. However, Rac1 directly regulates many other cellular events associated with the development of atherosclerotic plaque, including smooth muscle cell migration[203] and proliferation[204], and leukocyte–endothelial cell interaction[205]. Thus, the final outcome of the role of Rac1 in cardiovascular diseases is still controversial. Nevertheless, pathway-based genome-wide association analysis of coronary heart disease (CHD) has identified Rac1 as one of the biologically important genes in CHD, thus indicating that Rac represents a possible new

pharmacological target for cardiovascular diseases[206]. Thus from these evidence it appears clear that Rac1 represents a new potential pharmacological target for cardiovascular disease.

The purpose of the present study was to identify new and more active chemical entities capable to inhibit in a selective manner the Rac1 activity, and then study their effects in *in vitro* experimental models.

For the identification of new comopounds, in collaborations with Dott. Contini at the University of Milan, two approaches has been followed: 1) a virtual screening approach and 2) a computer aided de-novo design of a new scaffold, starting from the previously described 3D model of the complex between Rac1 and NSC23766 (see material and methods).

The identified compounds have been then screened in *in vitro* experimental model for their inhibitory activity on Rac and RhoA activation in response to PDGF-BB. The most promising compound were then utilized for the evaluation of their effect on cell migration and cell adhesion, Rac-mediated cellular events.

A second step of the present research project was then the analysis of the pharmacokinetic and pharmacodynamic profile of the Rac inhibitor identified and the development of an *in vivo* model of heart hypertrophy.

Materials and Methods

Virtual screening approach

The first inhibitor of Rac protein discovered was compound NSC23766 capable to interfere with the interaction between Rac and its activator GEF inhibiting its activation. This compound shows the capacity to inhibit Rac activity in a selective manner without affecting the activity of RhoA and Cdc42. However this compound resulted not very powerful with an IC_{50} of 50μM, moreover compound NSC23766 is not characterized by drug-like structure.

Starting from compound NSC23766 in our laboratory was denveloped another classes of rac inhibitors with the same mechanisms of action. In particular was found compounds **4** and **5** more active than compound NSC23766 with an IC_{50} of 24.1 and 12.2μM respectively[207].

Starting from this work the aim of our study was to identify new potent and selective compound capable to inhibit the Rac protein activation.

From the hit compounds **4** and **5**[207], a similarity search was performed directly on the ZINC DB website[208]. The clustering and search algorithms implemented in ZINC are based on a search engine provided by ChemAxon where both the query and molecules in the DB are represented by finger-prints, and the similarity degree is expressed as a Tanimoto coefficient (TC).

All the molecules with a TC value of ≥ 0.85 with respect to either compounds **1** (53 derivatives) or **2** (117 derivatives) were selected for molecular docking evaluation. As the receptor, the previously derived 3D model[207] was used and a consensus docking strategy using two different softwares, MOE and AutoDock4 (AD4)[209], and a total of three scoring functions (London dG and affinity,

implemented in MOE, and the default AD4 scoring function) was adopted as it proved to be a rather successful screening strategy[207]. Energies obtained by MOE and AD4 virtual screenings were compared and only those compounds for which the computed docking energies resulted above the defined thresholds (affinity < -4.5, London dG < -7.0, AD4 binding energy < -6.5 kcal mol-1) were selected. Within this selection, a total of 57 commercially available N- (sulfamoylaryl)arylamides with differences in regions 1 and 2 (Figure5) were selected and acquired for biochemical testing.

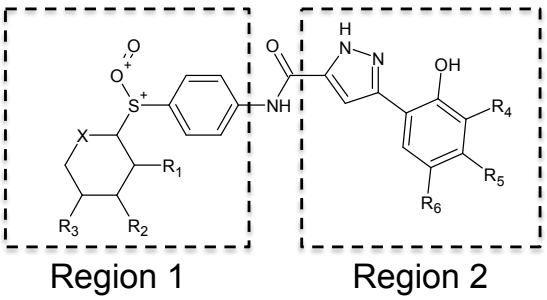

Figure 5: General chemical structure of new Rac inhibitors. Chemical modifications of the two indicated regions ledto the identification of a total of 57 commercially available *N*-(sulphamoylaryl) arylamides selected and acquired for biochemical testing.

Design and synthesis of arylsubstituted 2-amino-3-(phenylsulfanyl)norbornane-2-carboxylates as rac1-tiam1 protein-protein interaction inhibitors.

Aiming in prosecuting our research of novel and chemically diverse Rac1 inhibitors we decided to attempt a computer aided de-novo design of a new scaffold, starting from the previously described 3D model of the complex between Rac1 and NSC23766[210]. Thus, a series of derivatives based on the 2-

amino-3-(phenylsulfanyl)norbornane-2-carboxylate scaffold were synthetized for the pharmacological tests.

The use of the 2-amino-3-(phenylsulfanyl)norbornane-2-carboxylate scaffold for the design of potent and innovative Rac1 inhibitors acting at the protein-protein interaction interface between Rac1 and Tiam1 has been investigated. A binding mode analysis has been performed by docking followed by molecular dynamic simulations and MM-GBSA analysis, confirming that the norbornane scaffold can be conveniently used to prepare potent and selective Rac1 inhibitors[210].

Compounds.

Compounds selected from the virtual screening procedure were acquired from either Enamine (http://www.enamine.net/) or InterBioScreen (http://www.ibscreen.com/) and were guaranteed pure at 95% by both NMR and LC-MS analyses. The purity of compounds 1-25 was also verified by HPLC analysis and resulted above 98% (stationary phase Ascentis SI Supelco. 3 µm. 4.6 x 150.0 mm; mobile phase. n-hexane/ethanol 70:30; flow rate 0.7mL/min; detection UV 254. 270 and 290 nm). Chemical compounds were dissolved in DMSO to 10 mM final concentration and stored at 4 °C.

Reagents and antibodies.

DMEM, trypsin-EDTA, penicillin, streptomycin, non-essential amino acid solution, fetal calf serum (FCS), disposable culture flasks and petri dishes were purchased from Euroclone S.p.A. (Pero, Milan, Italy). Platelet derived growth factor-BB (PDGF-BB) was purchased from tebu-bio s.r.l. (Magenta, Milan, Italy). For western blot analysis, the following antibodies were used: mouse monoclonal anti-Rac1 (clone 23A8, Upstate), anti-mouse peroxidase-conjugated secondary antibodies (Jackson ImmunoResearch Lab; Cambridgeshire, UK). FITC-phalloidin was purchased from Sigma Aldrich (Milan, Italy).

Cell culture.

Human SMCs (A617 from human femoral artery) were grown in monolayers at 37 °C in a humidified atmosphere of 5% CO_2 in DMEM supplemented with 10% (v:v) fetal calf serum (FCS), 100 U/ml penicillin, 0.1 mg/ml streptomycin and non-essential amino acids. The medium was changed every third day. SMCs were identified for growth behavior, morphology and using monoclonal antibody specific for α-actin, the actin isoform typical of SMC. For the experiments cells were seeded at a density of $2x10^5$/35 mm petri dish and incubated with DMEM supplemented with 10% FCS; 24 h later the medium was changed to one containing 0.4% FCS, and the cultures were incubated for 48 h. At this time, the compounds were added to the cultured media and after 4 hours G-LISA assays or cell adhesion assay was performed.

RNA preparation and quantitative real time PCR analysis.

Total RNA was prepared from mouse heart tissues extracted with Macherey-Nagel DNA, RNA and protein purification kit according to manufacturer's instructions. For quantitative real time PCR reaction reverse transcription-polymerase first-strand cDNA synthesis were performed with 0.5 μg of total RNA, using iScriptTM cDNA synthesis Kit (BIO-RAD Laboratories, Hercules, CA, USA). Real time PCR were then performed using the Sybr Green QPCR Master Mix (Carlo Erba) and ABI Prism® 7000 Sequence Detection System (Applied Biosystems, Monza, Italy). mRNA expression levels of ANF (atrial natriuretic peptide), BNP (brain natriuretic peptide) and SMA (skeletal muscle actin) were normalized by using ribosomal 18S rRNA. PCR cycling conditions were as follows: 94°C for 3 minutes, 40 cycles at 94°C for 15 s, and 60°C for 1 min. Data were expressed as Ct values and used for the relative quantification of targets with the ΔΔCt calculation.

The primers utilized were the following:

mANF Forward: 5'-AGGAGAAGATGCCGGTAGAAGA-3'
mANF Reverse: 5'-GCTTCCTCAGTCTGCTCACTCA-3'

mBNP Forward: 5'-AGGGAGAACACGGCATCATT-3'
mBNPR Reverse: 5'ACAGCACCTTCAGGAGATCCA-3'

α-SMA Forward: 5'-TGTGCGCGACATCAAAGAG-3'
α-SMA Rev Reverse: 5'-GTGGCCATCTCATTCTCGAAA-3'

Cell migration assay.

The Boyden chamber and the polycarbonate membrane were purchased from Biomap (Agrate Brianza, Milan Italy). The membranes were coated with a 0.1

mg/ml of type I collagen solution (PureCol®, Nutacon BV, Leimuiden, The Netherlands) in 0.1 mol/L of acetic acid at 37°C for 24 h and washing twice with DMEM before cell seeding. The lower compartments of the wells of a modified Boyden chamber were filled (in triplicate) with DMEM containing 0.4% FCS in the absence or presence of PDGF-BB (20 ng/ml), whereas the upper compartments were filled with aliquots of the SMCs suspensions containing 106 cells/ml. The chamber was incubated at 37°C for 6 h. The membrane was then carefully removed. Adherent SMCs on the top were eliminated and the membrane was stained with the Diff-Quik staining set (Biomap, Agrate Brianza, Milan Italy). The number of transmigrated cells was then counted in four random high-power fields (HPFs) under high magnification (objective lens 20x). Data were presented as mean ± SD of the counted cells in triplicate wells.

Video microscopy analysis.

Time-lapse video microscopy was performed as described previously,65, 66 with slight modifications. In brief, cultured SMCs were placed on the stage of an inverted motorized microscope (Axiovert 200M Zeiss Instr., Oberkochen, Germany) in a cage incubator (CTI Controller 2700 digital Zeiss Instr., Oberkochen, Germany) at 37°C. Phase-contrast images were collected with a 10x A-Plan lens (Zeiss Instr., Oberkochen, Germany) every 15 minutes over a 16-h period using a camera (AxioCam HRm, Zeiss Instr., Oberkochen, Germany) and the Axiovision LE software (Zeiss Instr., Oberkochen, Germany).

Videos were generated using the ImageJ software for image analysis. Cell trajectories were determined using the manual tracking plugin of ImageJ (http://rsbweb.nih.gov/ij/download.html). This procedure generated x and y coordinates for the center of each cell at each time point. Trajectories were reconstructed according to the recorded data. The distance covered by each cell was extracted from the track plots. Ten cells from three independent experiments were analyzed for each condition, and data were expressed as mean ± SD.

G-LISA assay for Rac1 and RhoA.

The intracellular amount of Rac1-GTP and RhoA-GTP were determined by using the G-LISA assay (Cytoskeleton, Inc Denver, CO, USA). The GLISA™ assay uses a 96-well plate coated with RBD domain of either RhoA or Rac1. The active GTP-bound form of Rho protein, but not the inactive GDP-bound form, from a total cell lysates of human cells, binds to the plate. Bound active Rho protein was then detected by incubation with a specific primary antibody followed by a secondary antibody conjugated to horseradish peroxidase (HRP). The signal is then developed with OPD reagents.

Cytoskeleton staining.

Cells were fixed in 4% paraformaldehyde at room temperature for 10 min, permeabilized in 0.1% Triton X-100 in PBS for 5 min, and incubated with FITC-phalloidin (Molecular Probes). Cells were then washed four times with PBS,

incubated with DAPI solution for 5 min, and coverslipped with vectashield mounting media. Cytoskeleton staining of cells was analyzed by fluorescent microscope.

Cell adhesion assay.

Adhesion studies were performed as described previously[211]. Briefly, SMCs were harvested with Trypsin-EDTA after 4h incubation with increasing concentrations of tested compounds, centrifuged and resuspended in DMEM with 0.4% FCS and plated into 96 well/plates at 100,000 cells/well. Plates were incubated for 15 min at 37 °C in the incubator, and the assay was terminated by rinsing the plates with PBS and fixing the cells with 4% paraformaldehyde. Cells were stained with 0.5% toluidine blue for 1 min and rinsed in water. They were then solubilized by the addition of 1% SDS and quantitated in a microtiter plate reader at 595 nm.

Western blot analysis.

Cells were lysed with a solution of 50 mM Tris pH 7.5, 150 mM NaCl, 0.5% Nonidet-P40, containing a protease and phosphatase inhibitor cocktails (Sigma Aldrich, Milan, Italy). Equal amount of total protein per sample were separated by SDS-PAGE under reducing conditions, transferred to Immobilon PVDF (GE Healthcare Little Chalfont, Buckinghamshire, UK) and subsequently immunoblotted with antibody anti Rac1 (Clone 23A8, Millipore) following appropriate secondary antibody, prior to visualization by enhanced

chemiluminescence (LiteAblot Extend Long Lasting Chemiluminescent Substrate, EuroClone)[212].

Transfection of siRNA.

The siRNAs directed to Rac1 was from Ambion life technologiesTM (Silencer Select Pre-designed siRNAs)[203]. Transfections were performed using siLentFectTM Lipid Reagent. (BIO-RAD laboratories, Hercules, CA, USA) according to the manufacturer's protocol[213]. SMCs were seeded at a density of 2×10^5/Petri dish (35 mm) the day before the transfection in 10% FCS DMEM. Cells were then transfected with 20 nM of siRNA for 24 h then the medium replaced with DMEM containing 0.4% FCS for an additional 24 h before performing the adhesion assay assay.

Transfection of plasmid encoding GEFs.

Tiam1 vector was kindly provided by J. Collard (Cancer Institute, Amsterdam, The Netherlands); TrioN vector was from P. Fort (Centre de Recherche de Biochimie Macromoléculaire, Universités Montpellier I et II, France) and Vav2 vector from X. Bustelo (Centro de Investigación del Cáncer-Cancer Research Center, CSIC-University of Salamanca, Spain). Transfections were performed using jetPEI transfection reagent (Polypus-transfection SA, Illkirch, France) according to the manufacturer's protocol. SMCs were seeded at a density of 2×10^5/Petri dish (35 mm) the day before the transfection in 10% FCS DMEM. Cells were then transfected for 24 h then the medium replaced with DMEM

containing 0.4% FCS for an additional 24 h. Cells were then incubated with compound 2 and Rac-GTP levels determined by G-LISA assay after 4 h.

Statistical analysis.

All data shown are representative of at least three replicate experiments. Data are expressed as mean±SD. Statistical analyses were performed using the unpaired Student's T test. P values <0.05 were considered significant. The concentration of compounds required to inhibit 50% of Rac-GTP intracellular levels (IC_{50}) was calculated by nonlinear regression curve (SigmaPlot software; Systat Software, Inc., Point Richmond,CA).

Determination of plasma levels of Rac inhibitor compound 4.

For the pharmacokinetics analysis was used as a stationary phase C18 column of 15cm and a mobile phase consisting of a mixture of A 99,9% of H2O and 0,1% ammonium formate and one of B of 99,9 % acetonitrile and 0,1% of mixture A.

The two solutions were then mixed with the following gradient protocol:

- Time 0: 90% A + 10%B
- 6 min: 10% A + 90% B
- 10 min: 2% A + 98% B
- 15 min: 2% A + 98% B
- 15.10 min: 90% A + 10% B

Final Time: 30 min.

Flux: 0,25 mL/min

Before performing the experiment on plasma samples we performed the construction of the standard scale melting at concentrations of 0.3125, 0.625, 1.25, 2.5 and 5ng of compound **4** in acetone (Figure6).

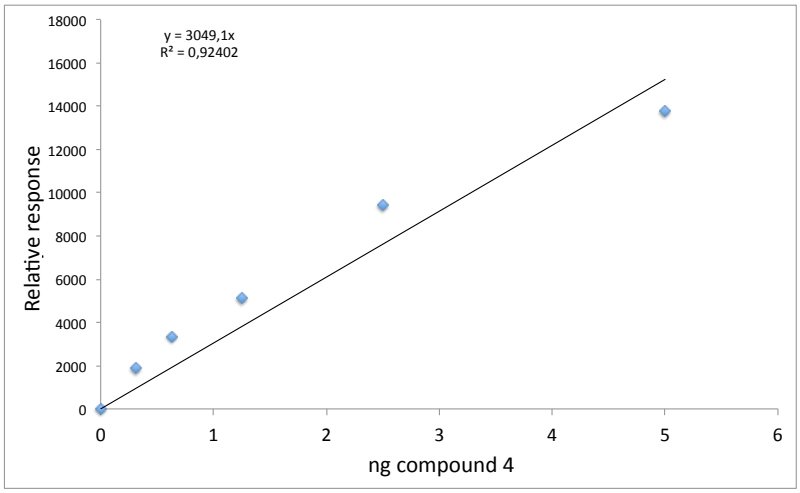

Figure 6: Evaluation of the compound 4 with known concentrations of human plasma. The plasma was prepared with 0.01% EDTA to prevent coagulation. Centrifuged for 20 minutes at 3000 rpm. Plasma was added in volumes of 200 µl to which was added.

- Increasing concentrations of compound **4** (0.3 ng to 5ng) dissolved in acetone.
- The volume of plasma thus obtained was brought to 800 µl with acetone to precipitate all the plasma proteins.
- The samples was at 4°C O/N for the separation of idrophilic and lypophile phases
- The precipitate was removed by centrifugation for 10 minutes at 15,000 rpm at 4 ° C.

- The supernatant was transferred to new Eppendorf and evaporated by SpeedVac for 1-2 hours.

The residue was resuspended in 50 µl of solution B and 100% of 10 µl injected in Mass.

A second step of the pharmacokinetic study has been to build the regression line of the compound stocks-58132 as an internal standard.

The construction of the line was made by injecting into the column increasing concentrations of the compound from 0.315ng up to 2ng.

The regression line was then utilized to evaluate the performance of our method starting from mouse plasma samples with 5ng of internal standard. An analysis carried out it was possible to calculate a yield of about 30% (Figura 7).

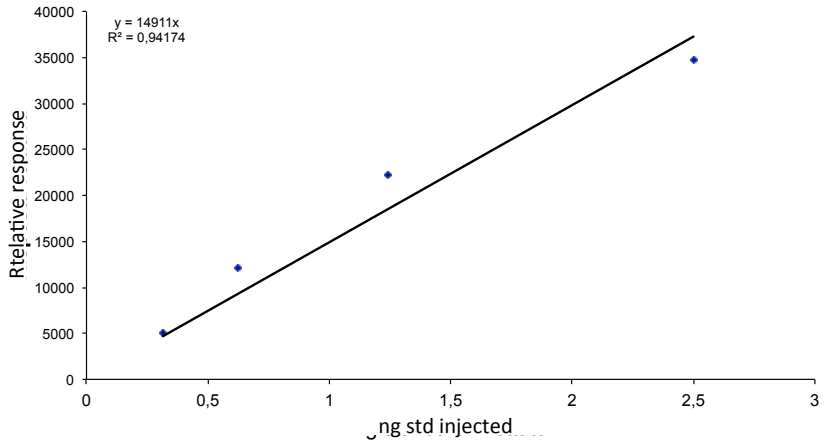

Figure 7: Linear regression analysis of the internal standard

Later we assessed the concentration of the compound **4** present in the plasma of mice after i.p. administration at a concentration of 50 mg/kg/day. Taking into account the performance of our method of preparation we calculated that the plasma concentration of the compound **4** was 1.4 nM.

In vivo MRI.

A 3.8 cm diameter birdcage resonator was used on the same 15cm 4.7 T vertical magnet. Mice were anesthetized with 2% isofluorane (Abbot) in N_2/O_2 (70%/30%) using a vaporizer. The anaesthetic was delivered through a face mask, and temperature of animals was maintained around 37-38°C. The left ventricular section was visualized using T2 weighted sequences (TE=80ms, TR=3s, FOV=3cm^2, in-plane resolution=234µ^2, slice thickness=1mm, number of slice=6-7).

Results

Pharmacological evaluation of compounds identified by the virtual screening approach.

To induce Rac activation, human SMCs were starved for 48h in DMEM containing 0.4% FCS and then stimulated for 2 min with 20 ng/mL with PDGF-BB. The effect of tested compounds was assessed by pre-incubating human SMC for 4h before stimulation. In the first series of G-LISA assays, a final non-toxic concentration (between 10 and 200 µM) of the 57 selected compounds was utilized, as determined by MTT cytotoxicity assay. Among the 57 tested compounds, 23 efficiently reduced the intracellular content of Rac-GTP from a minimum of 24.8% to a maximum of 63.7%. Importantly, five compounds were shown to be more effective than the reference compound **1** and fifteen were more effective than compound **2**, indicating a potential improvement of the pharmacological inhibition of Rac by the newly identified chemical entities.

A second series of analyses was performed at 25 µM concentration in order to select the most potent compounds (Figure 8).

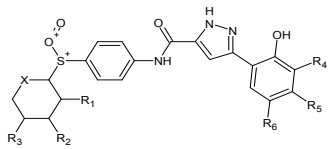

cmpd	R^1	R^2	R^3	R^4	R^5	R^6	X	% inhibition at 25 µM
21	H	CH_3	H	CH_3	CH_3	H	$-CH_2-$	68.3±6.3 ***
3	H	CH_3	H	H	H	H	$-CH_2-$	67.4±1.5 ***
11	H	CH_3	H	H	CH_3	H	$-CH_2-$	65.3±9.0 ***
4	H	H	H	H	H	H	$-CH_2-$	61.1±3.0 ***
5	H	H	H	CH_3	CH_3	H	$-CH_2-$	59.3±1.2***
6	H	H	CH_3	H	H	H	$-CH_2-$	51.9±3.1**
10	H	H	CH_3	CH_3	CH_3	H	$-CH_2-$	46.5±17.7 ^{NS}
20	H	H	CH_3	CH_3	H	CH_3	$-CH_2-$	45.5±24.2 *
14	H	H	H	CH_3	CH_3	H	$-CH_2-CH_2-$	40.8±21.4*
16	H	H	H	H	CH_3	H	$-CH_2-CH_2-$	26.1±3.8 ***
24	H	H	CH_3	H	CH_3	CH_3	$-CH_2-$	21.9±0.2 ^{NS}
15	H	H	H	H	H	H	$-CH_2-CH_2-$	NE

NE: Not effective; NS: Not significant

*p<0.05; **p<0.01; ***p<0.001 Student's T-test.

Figure 8: Inhibitory effect of the first 12 most potent compounds on Rac activity. SMCs were incubated with selected compounds at final concentration

of 25 μM for 4 hours and then Rac-GTP levels was determined with G-LISA assay.

Compounds **3**, **4**, **5**, **11** and **21** showed the most potent inhibitory action on Rac protein and consistently reduced, by more than 50%, the intracellular amount of Rac-GTP. A dose dependent effect on Rac activity showed that compounds **5** and **4** have the lowest IC_{50} values, 4.4 μM and 8.7 μM, respectively[214].

In order to determine the selectivity of action of the tested compounds on Rac, the G-LISA assay specific for RhoA was performed.

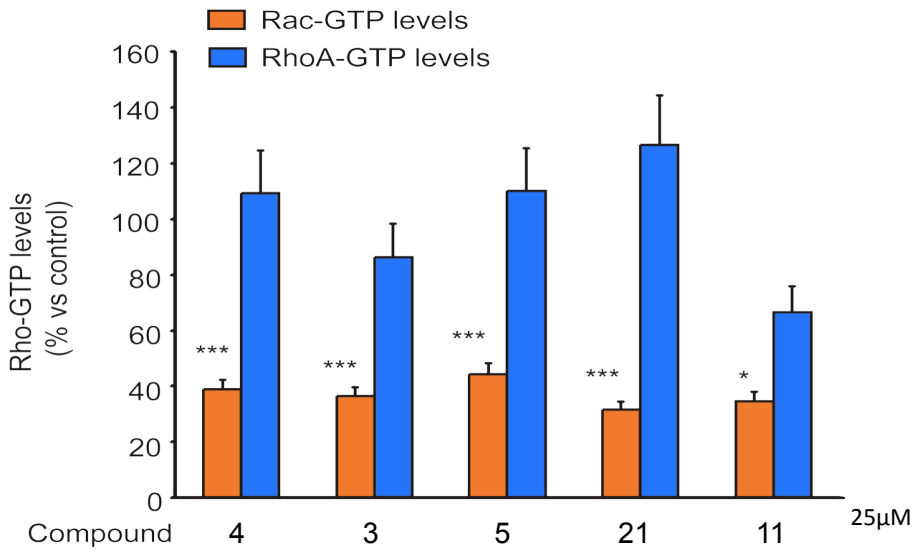

Figure 9: Effect of compound 4 on Rac and RhoA activity in SMCs. SMCs were incubated with selected compounds at final concentration of 25 μM for 4 hours and then Rho-GTP levels was determined with G-LISA assay.

As shown in Figure 9, compounds **3**, **4**, **5**, and **21** strongly reduced the intracellular levels of Rac-GTP without significantly affecting the activity of RhoA, while compound **11** appears to be less Rac-selective.

From the five most potent compounds we preformed a curve dose-response and then calculated the IC_{50} (Figure 10).

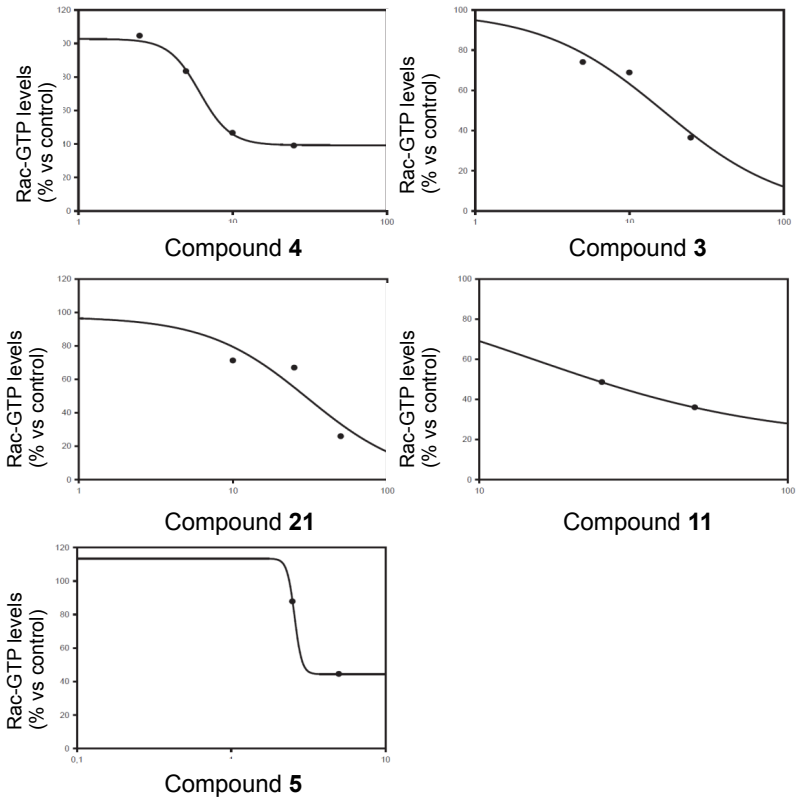

Figure 10: Concentration-dependent Rac inhibitory activity of selected compounds. Rac1 activity was determined after incubation with increasing concentrations of selected compounds and then evaluated by G-LISA assay. IC_{50} values were then calculated by using Sigma Plot software.

In the table3 we calculated the IC_{50} of the five compounds, in particular, compounds **4** and **5** show an IC_{50} lower than the starting compounds. Furthermore the compound **4** shows a modular dose response curve. Since compound **4** showed a good dose response curve and a good selectivity, it was considered the best candidate for further *in vitro* and *in vivo* studies.

Compounds		Rac1-GTP $IC_{50}(\mu M)$
5	Stocks-37744	4.4 ± 3.1
4	Stocks-26339	8.7 ± 2.4
3	Stocks-48446	16.4 ± 2.1
11	Stocks-50919	19.2 ± 2.8
21	Stocks-51425	29.1 ± 5.1

Table 3: IC_{50} values of selected compounds on Rac1 inhibitory activity

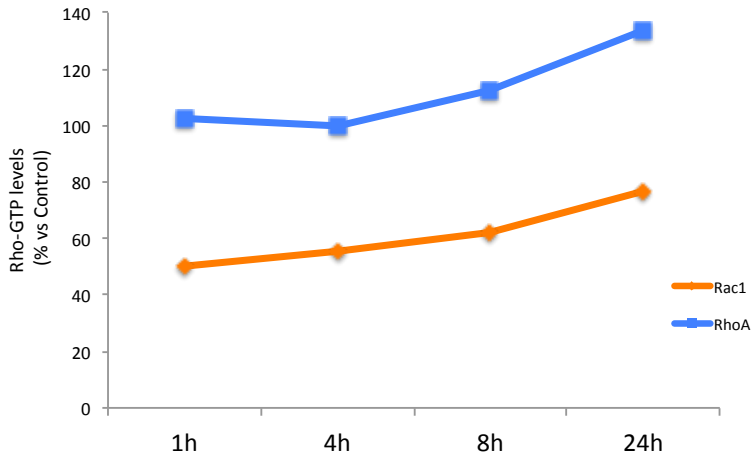

Figure 11: Time-dependnet Rac inhibitory activity of compound 4. Cells were seeded at a density of $2x10^5$/35 mm petri dish and incubated with DMEM supplemented with 10% FCS; 24h later the medium was changed to one containing 0.4% FCS, and the cultures were incubated for 48h. At this time, compound 4 (25 µM) was added to the cultured media. Total cell lysates were then prepared after 0 (control) 1, 4, 8 and 24 h and the levels of GTP-bound forms of Rac and RhoA determined by G-LISA assays. ***p<0.001; **p<0.01 vs Control

The time-dependent effect of compound **4** clearly demonstrated that its inhibitory effect on Rac is selective and very rapid with a significant reduction of Rac-GTP after 1 h of incubation (Figure11). This effect appears to be stable up to 6-8 hours and losing some activity after 24h from the incubation.

To investigate the basic molecular mechanism of Rac inhibition, we examined the effect of compound **4** on the exchange activity of Tiam1 and TrioN, Rac-specific GEFs[215,216] and Vav2, a GEF active on Rac1, RhoA, and Cdc42[217]. The treatment with compound **4** strongly reduced the Rac1-GTP levels induced by SMCs expressing either Tiam1, TrioN, or Vav2[214]. These results indicate that compound **4** interferes with the GEF-mediated Rac activation (Figure12).

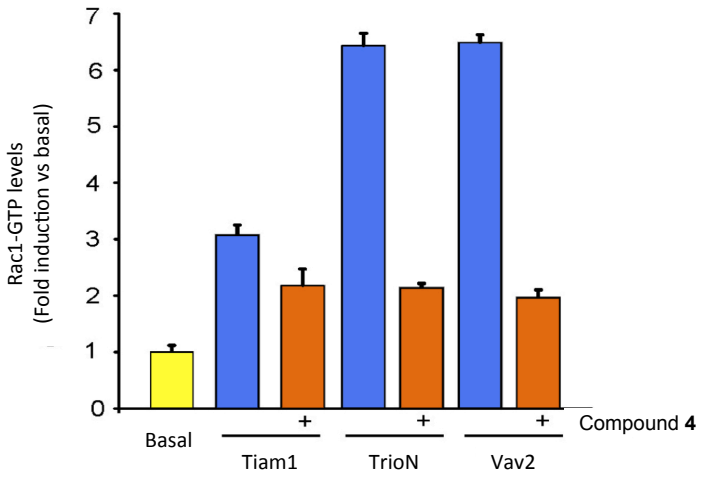

Figure 12: Effect of compound 4 on GEF-mediated Rac activation in SMCs. SMCs were transiently transfected with plasmids encoding for either Tiam1, TrioN or Vav2 and incubated for 4h with Compound **4** (25µM) in DMEM containing 0.4% FCS. At the end of the incubation Rac1-GTP levels were determined by G-LISA assay.

To delineate the anti-Rac activity of the selected compounds in cultured cells, their effect on Rac1-dependent cell adhesion was evaluated. Rac activity has been previously shown to be required for cell adhesion[218], and its downregulation by siRNA directed to Rac1 strongly reduced the capability of cells to adhere to the Petri dish (Figure13).

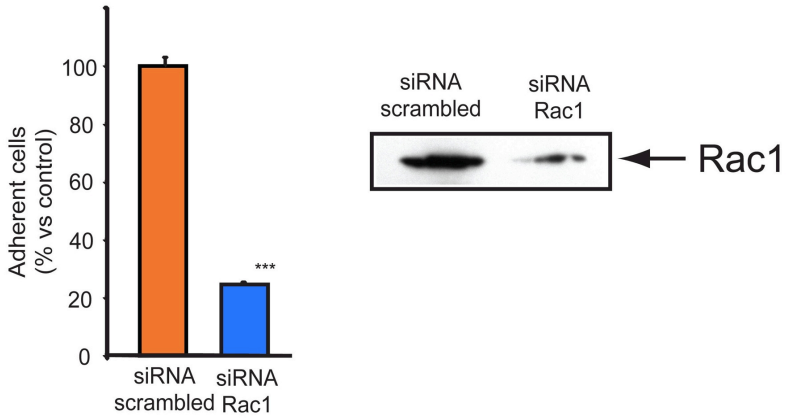

Figure 13: Effect of downregulation by siRNA directed to Rac1 on SMC adhesion. Cells were seeded at a density of $2x10^5$/35 mm petri dish and incubated with DMEM supplemented with 10% FCS; 24 h later the cells were transfected with siRNA against Rac1 or nonsilencing control siRNA scrambled. A) After 24h SMCs were starved with medium containing 0.4% FCS for an additional 24h. At this time, the cells were harvested with Trypsin-EDTA and cell adhesion on cultured petri dish evaluated. B) A parallel set of petri dishes were utilized for the determination of Rac1 expression by western blot analysis with a monoclonal antibody anti Rac1 (Clone 23A8, Millipore).

The effect of the five selected new Rac inhibitors on cell adhesion was then determined. SMCs were incubated for 4 h with increasing concentrations of compounds (10–50 μM), harvested by trypsinization, and then cell adhesion was determined. All the compounds were capable of significantly affecting cell adhesion in a concentration-dependent manner[214] (Figure14). In particular, compounds **4**, **11** and **21** showed very similar IC_{50} values on the cell adhesion and the inhibitory action on Rac, demonstrating the effective inhibition of a Rac-mediated cellular event by these compounds.

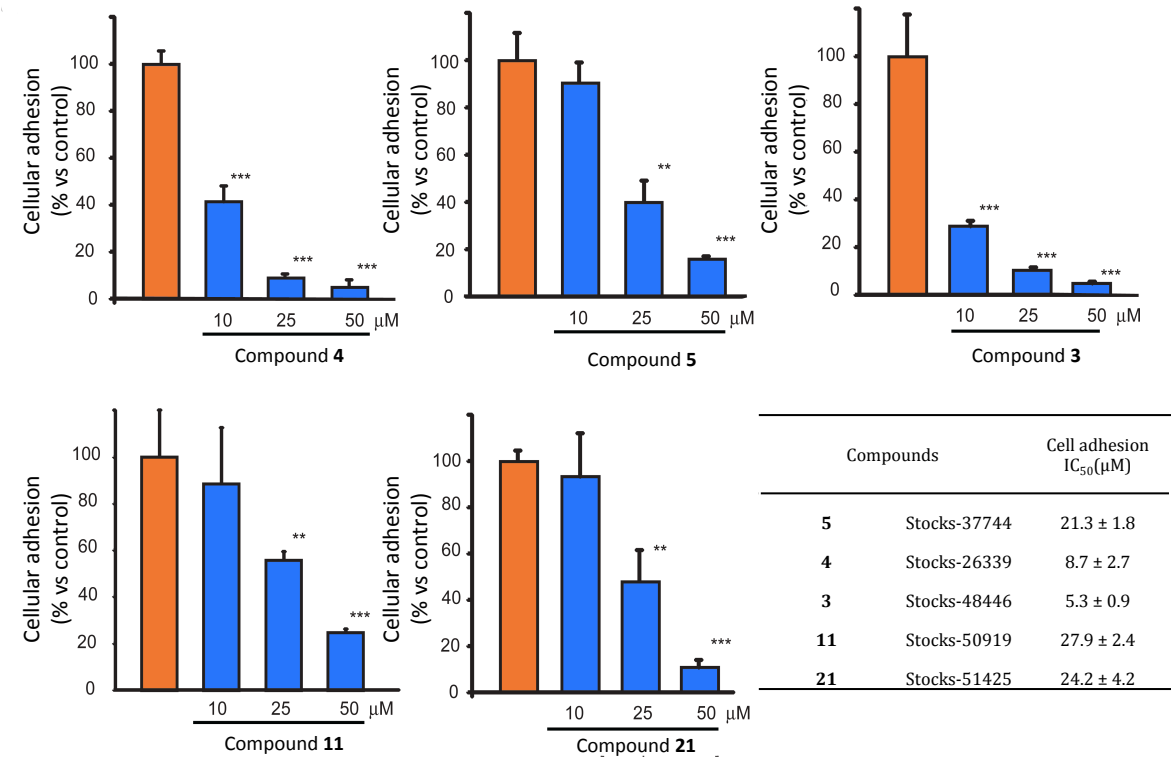

Compounds		Cell adhesion IC_{50}(μM)
5	Stocks-37744	21.3 ± 1.8
4	Stocks-26339	8.7 ± 2.7
3	Stocks-48446	5.3 ± 0.9
11	Stocks-50919	27.9 ± 2.4
21	Stocks-51425	24.2 ± 4.2

Figure 14: Effect of selected compounds on SMC adhesion. Cells were seeded at a density of $2x10^5$/35 mm petri dish and incubated with DMEM supplemented with 10% FCS; 24h later the medium was changed to one containing 0.4% FCS, and the cultures were incubated for 48h. At this time, the compounds were added at indicated final concentrations to the cultured media and after 4h harvested with Trypsin-EDTA and cell adhesion on cultured petri dish evaluated.

A second cellular function, beyond cell adhesion, that is strickingly influenced by Rac activity is the cell migration in response to PDGF. Moreover, such event is considered a pivotal feature of atherosclerotic plaque development. For this reason we tested the effect of compound **4** on PDGF-mediated smooth muscle cell migration by both Boyden chamber chemotactic assay and video-micrscopy analysis.

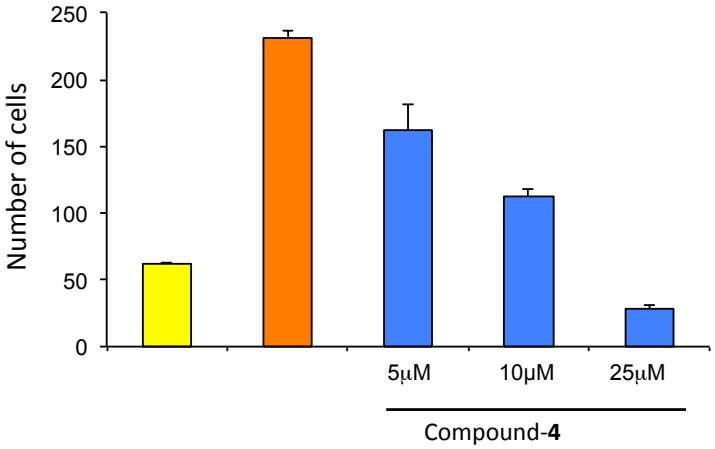

Figure15: Effect of compound 4 on SMC migration assessed by Boyden chamber. The cells were seeded on top of the chamber in the presence or absence of compound **4** at increasing concentrations. As stimulus mitogen was added at the lower part of the chamber of 20ng/ml PDGF-BB. After 6 hours of migration membrane was fixed, stained cells and their number determined in the microscope with a magnification of 10X.

As shown in Figure 15, compound **4** significantly inhibited cell migration in a concentration-dependent manner with a calculated IC_{50} value of 8.8 μM (Figure15).

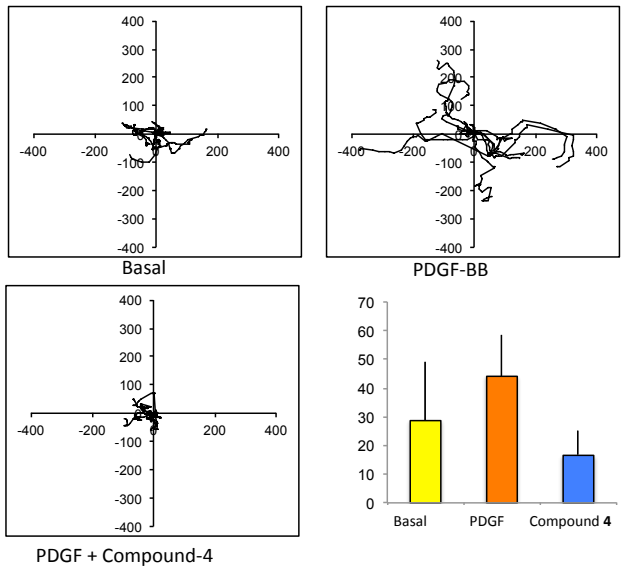

Figure16: Effect of compound 4 on SMC motility in response to PDGF-BB. SMCs were seeded at a density of $2x10^4$ of 24 well tray and incubated with DMEM supplemented with 10% FCS; 24h later the medium was changed to one

containing 0.4% FCS, and the cultures were incubated for 48 h. At this time, compound **13** was added to the cultured media at the final concentration of 10 μM in the presence of PDGF-BB (10 ng/ml). Cell movement was determined by video microscopy analysis and the distance covered by 10 different cells in 16 h was measured for each condition. The data are expressed as mean ± SD.

To confirm that compound **4** inhibits cell migration, we performed a second experiment on cell motility by video microscopy analysis conducted in the presence of PDGF-BB for 16hrs (Figure16). Under these experimental conditions compound **4** significantly affected cell motility with an IC_{50} value of 1.75 μM. Finally, compound **4** was shown to inhibit lamellipodia formation in human SMCs induced by PDGF-BB (Figure17), a cellular response strikingly related to Rac1 activity[214].

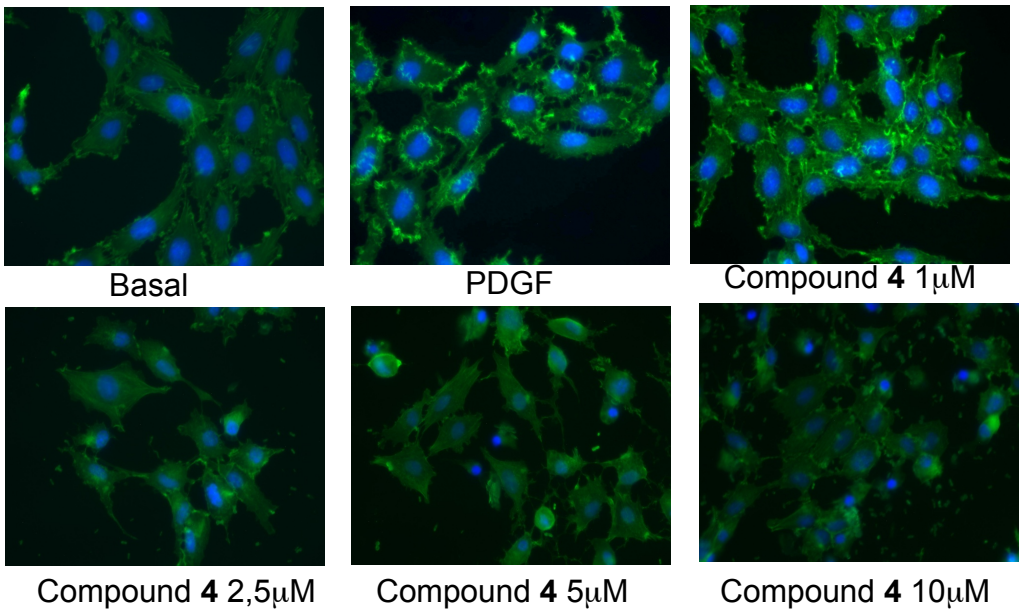

Figure17: Effect of compound 4 on cytoskeleton organization. Cells were incubated with Compound **4** at the final concentration of 10μM and after 4h SMCs were stimulated by adding PDGF-BB (10 ng/ml) for 10min. Cells were then fixed in 4% paraformaldehyde and labeled with FITC-phalloidin and analyzed by fluorescent microscope.

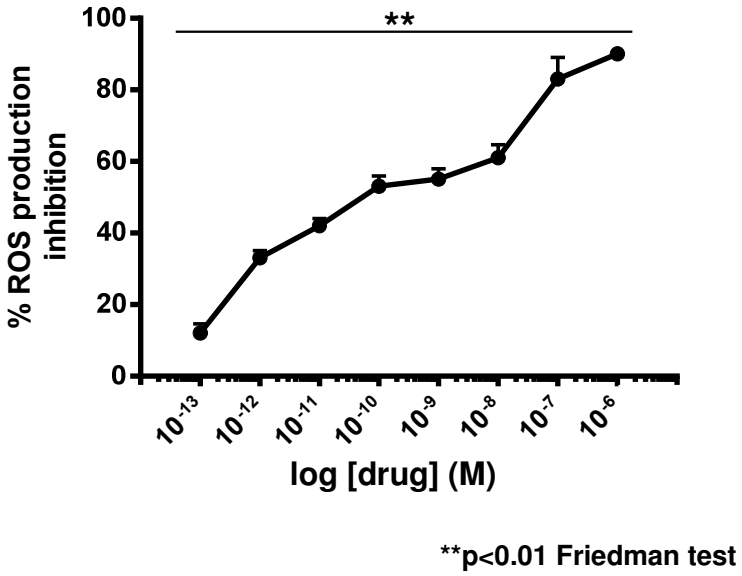

Figure18: **Effect of compound 4 on ROS production in human monocytes.** To evaluate superoxide anion (O2-) production, monocytes (1 x 10^6 cells/ plate) were first treated for 1 h with compound 4 and then stimulated with PMA 10^{-7} M for 30 min. O2- production was evaluated by the superoxide dismutase (SOD)-inhibitable cytochrome C reduction assay and expressed as value of PMA-induced ROS production inhibition. The absorbance changes were recorded at 550 nm in a Beckman DU 650 spectrophotometer. To avoid interference with spectrophotometrical recordings of $O2^-$ production, cells were incubated with RPMI 1640 without phenol red, antibiotics and FBS.

Rac1 is very important for the activation of NADPH oxidase and thus has a pivotal role in the production of ROS. With the cytochrome C reduction assay we evaluated the effects of compound **4** on superoxide anion production in human monocytes. Compound **4** significantly inhibited the ROS production with an IC_{50} of 1nM (Figure 18). These results further demonstrate that compound **4** inhibits Rac activity eliciting a potential antioxidant activity.

Pharmacological evaluation of arylsubstituted 2-amino-3-(phenylsulfanyl)norbornane-2-carboxylates on Rac1 activity.

The second series of compounds with potential Rac inhibitory activity derived by a different approach (see material and methos) were tested under the same experimental conditions reported for the previous series. As shown in (Figure 19), all the compounds significantly reduced the intracellular levels of Rac-GTP at 10μM concentration, and compound **13** reduced the levels of Rac-GTP by 75% compared to control cells[210]. At the same concentration, the compound did not interfere with RhoA activation, demonstrating a selective action towards Rac protein, moreover compound **13** affects cell migration and motility capacity in response to the chemotactic response to PDGF-BB.

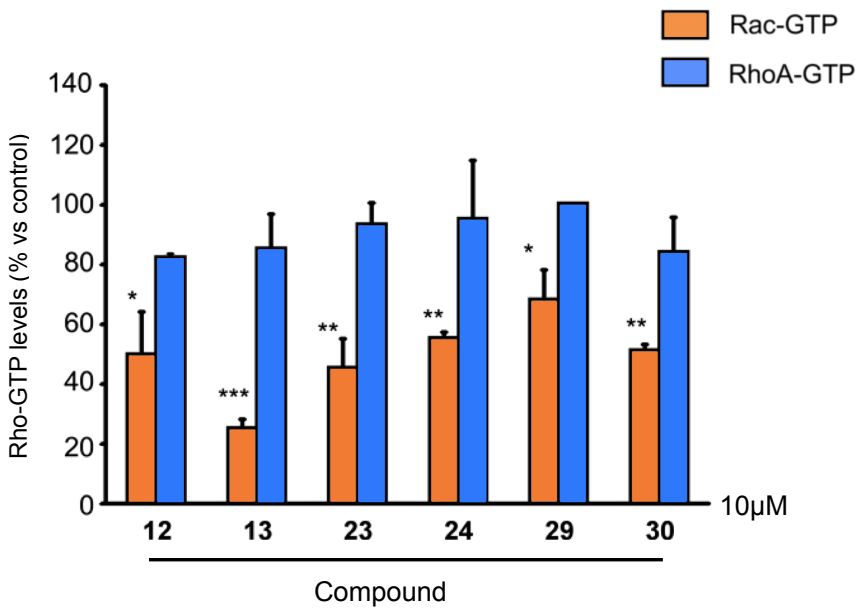

Figure 19: Effect of newly synthesized compounds on Rac-GTP and RhoA-GTP levels in SMCs stimulated with PDGF-BB. SMCs were seeded at a density of $2x10^5$/35 mm petri dish and incubated with DMEM supplemented with 10% FCS; 24h later the medium was changed to one containing 0.4% FCS, and the cultures were incubated for 48 h. At this time, the compounds were added to the cultured media at the final concentration of 10 μM and after 4 h Rac and RhoA activation was induced by PDGF-BB (20ng/ml) for 2 min. Total

protein extracts and G-LISA assays were then performed. The data are expressed as mean ± SD of triplicates.

In particular, compound **13**, selectively reduced the Rac-GTP levels in a concentration dependent-manner with an IC_{50} value of 2.5 μM with no effect on RhoA (Figure 20).

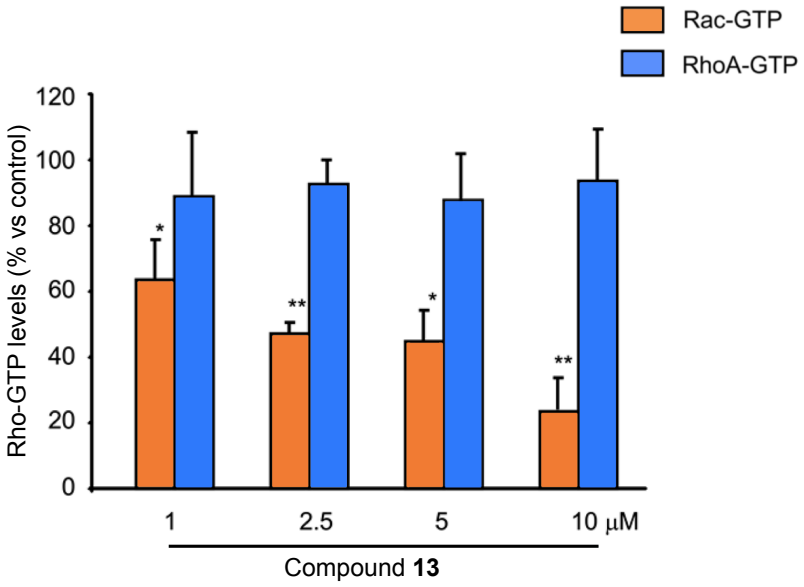

Figure 20: Effect of compound 13 on Rac-GTP and RhoA-GTP levels in SMCs stimulated with PDGF-BB. The experimental conditions were the same as those described in Figure 5 with the exception that the final concentrations of compound **13** were 1, 2.5, 5, and 10 μM.

Incubation of SMCs with increasing concentration of compound **13** (5-25 μM) determined a significant reduction of cell migration (Figure 21). In particular, at 25 μM compound **13** completely inhibited the chemotactic effects of PDGF-BB bringing the number of migrated cells to that observed under basal condition.

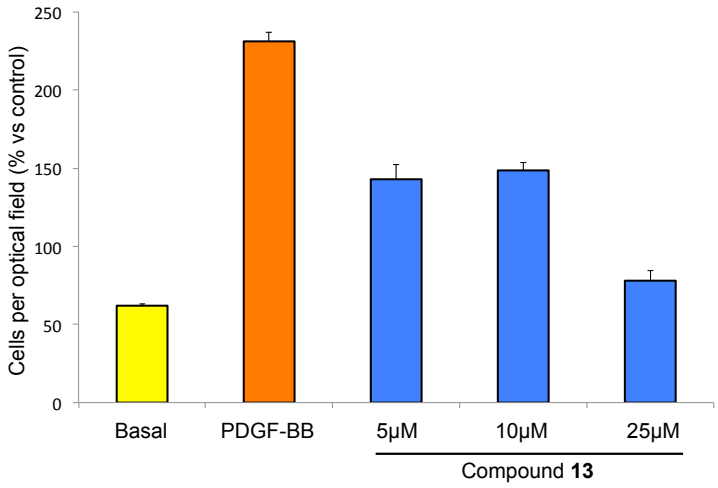

Figure 21: Effect of compound 13 on SMC migration in response to PDGF-BB. SMCs were seeded at a density of $2x10^5$/35 mm petri dish and incubated with DMEM supplemented with 10% FCS; 24h later the medium was changed to one containing 0.4% FCS, and the cultures were incubated for 48h. At this time, compound **13** was added to the cultured media at the indicated final concentrations. After 4h of incubation cells were harvested with trypsin, and cell migration determined by the Boyden chamber chemotaxis assay towards PDGF-BB (20 ng/ml). The number of transmigrated cells was counted in three random high-power fields under high magnification (×20 objective lens). The data are expressed as mean ± SD of triplicates.

The effect of compound **13** was also assessed on the mobility of SMCs by monitoring with a video microscopy (Figure 22). During the 16 h of video microscopy analysis, PDGF increased by approximately 2 fold the cell motility and this response was completely abrogated by the incubation with compound **13** at 10 μM concentration.

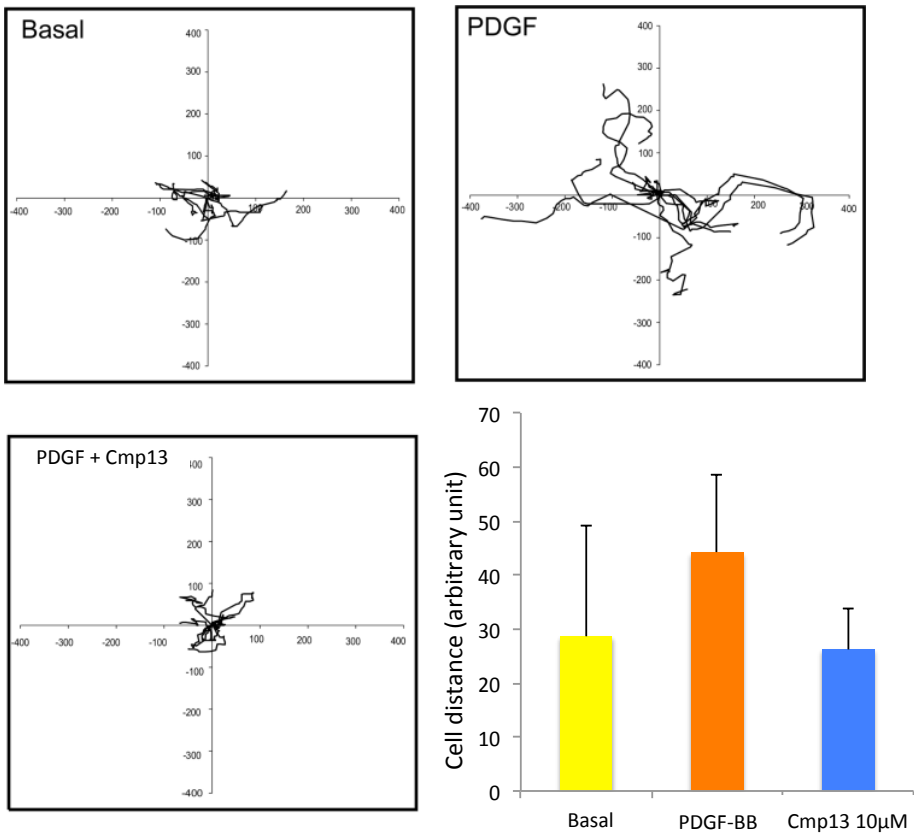

Figure 22: Effect of compound **13** on SMC motility in response to PDGF-BB. SMCs were seeded at a density of $2x10^4$ of 24 well tray and incubated with DMEM supplemented with 10% FCS; 24h later the medium was changed to one containing 0.4% FCS, and the cultures were incubated for 48 h. At this time, compound **13** was added to the cultured media at the final concentration of 10 µM in the presence of PDGF-BB (10 ng/ml). Cell movement was determined by video microscopy analysis and the distance covered by 10 different cells in 16 h was measured for each condition. The data are expressed as mean ± SD.

Taken together the compound **13** was shown to selectively reduced the intracellular levels of Rac-GTP and the cell migration, an event dependent by its activity[210].

In vivo pharmacokinetic and pharmacodynamic study in C57 BL/6 mice.

Once identified in compound **4** the best candidate for the in vivo evaluation on cardiac hypertrophy and atherosclerosis, in a first series of experiments both the pharmacokinetic and the pharmacodynamics profile were determined. For these analysis compound **4** was administered in C57BL/6 mice at a dose of 50 and 100 mg/kg/day (i.p. injection of CMC suspension) for three days and after the last injection both the plasma levels of compound **4** and the cardiac levels of Rac-GTP were determined.

After the last administration the compound at a dosage of 50 mg/kg/day it was observed a 35% reduction of Rac-GTP levels in cardiac homogenates at 1h together with a Cmax of 925 ng/ml , while at a dose of 100mg/kg/day we observed a Cmax of 2050 ng/ml after 3h with a reduction of 98% of Rac-GTP (Figure 21 and 22).

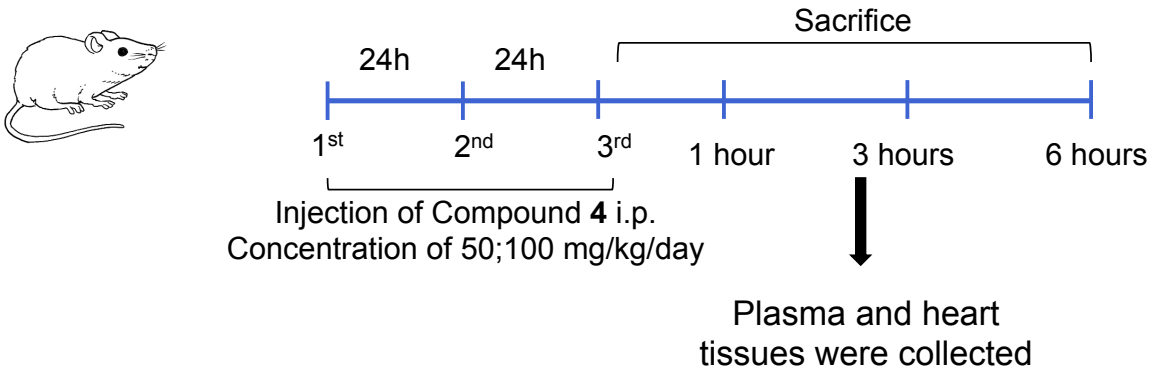

Figure 21. Experimental protocol for pharmacokinetic and pharmacodynamic studies.

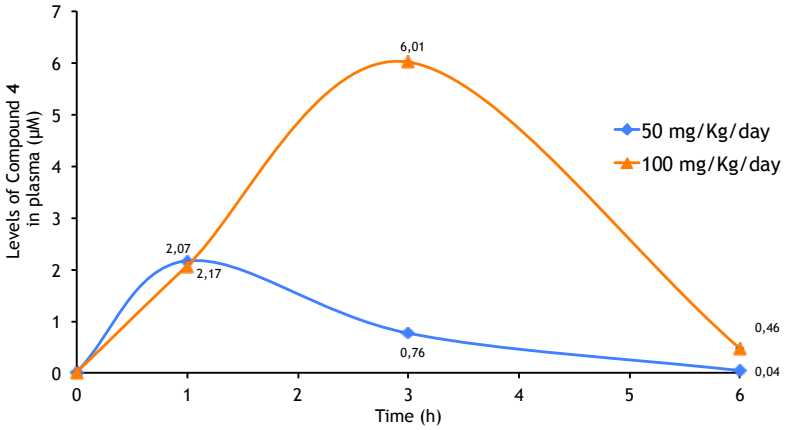

Figure 23: Plasma levels of compound 4. Compound **4** was administered every 24h for 3 days by i.p. at 50 and 100mg/kg per day. The Compound **4** levels in plasma were evaluated by HPLC-MS after 1, 3 and 6 hours from last administration.

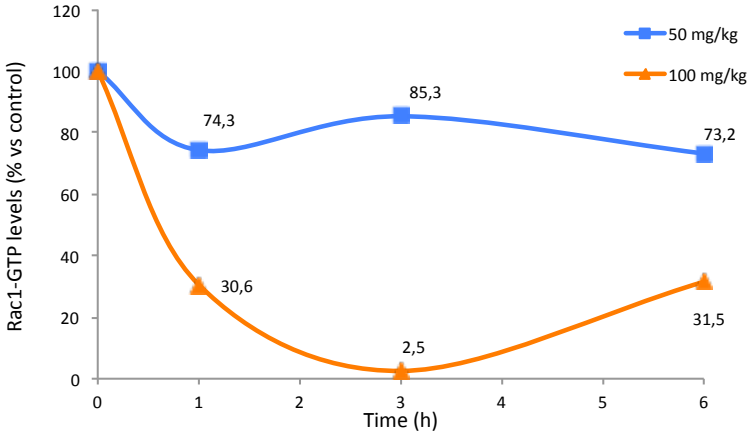

Figure24: Rac1-GTP levels in mouse heart after compound 4 administration. Compound **4** was administered every 24h for 3 days by i.p. at 50 and 100mg/kg/day. The Rac-GTP levels were evaluated by G-LISA assay after 1, 3 and 6 hours from last administration of Compound **4** in hearts of C57 BL/6 mice.

Taken together a very nice correlation between the plasma concentrations and the cardiac Rac inhibition was observed with a more pronounced and slower action at higher dose 100 mg/kg per day compare to the lower (Figure24).

Moreover, the pharmacokinetic analysis clearly showed that the compound **4** does not accumulate in the body but is rapidly excreted (Figure23).

Characterization of heart hypertrophy model.

Before starting with the *in vivo* study of compound **4** we characterized a mouse model of heart hypertrophy induced by infusion of Angiotensin II through osmotic pump (alzet 1004) at a concentration of 1000 and 2000mg/kg/min.

We treated the mice for 2 weeks with Angiotensin II and, at the end of each week, we monitored by MRI the volume of Left ventricle, fraction of ejection and collected plasma to measure the concentration of AngII in plasma.

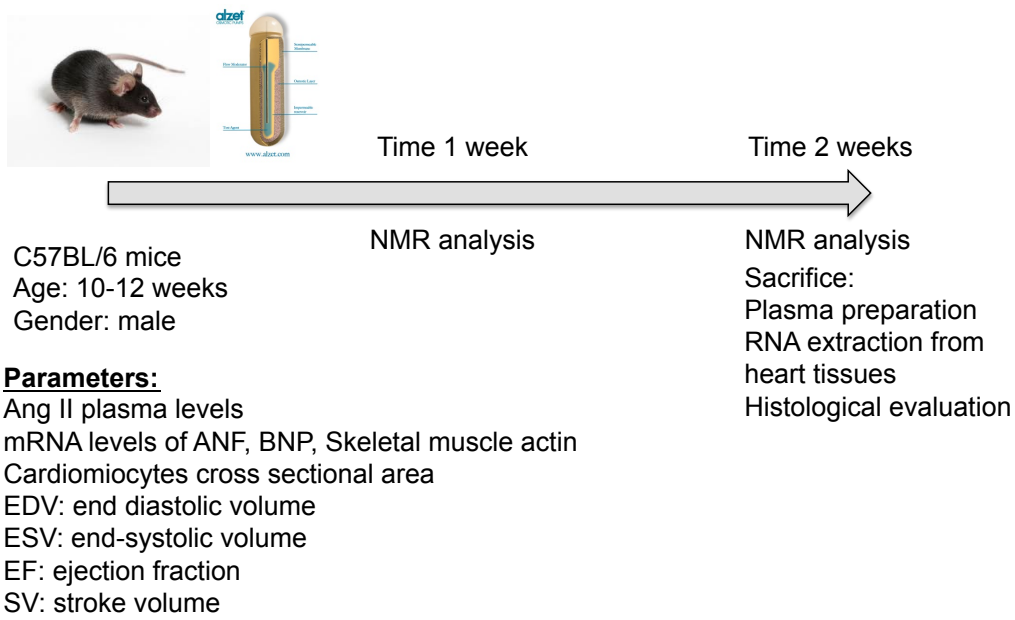

Figure 25: Experimental protocol of heart hypertrophy induced by angiotensin-II infusion.

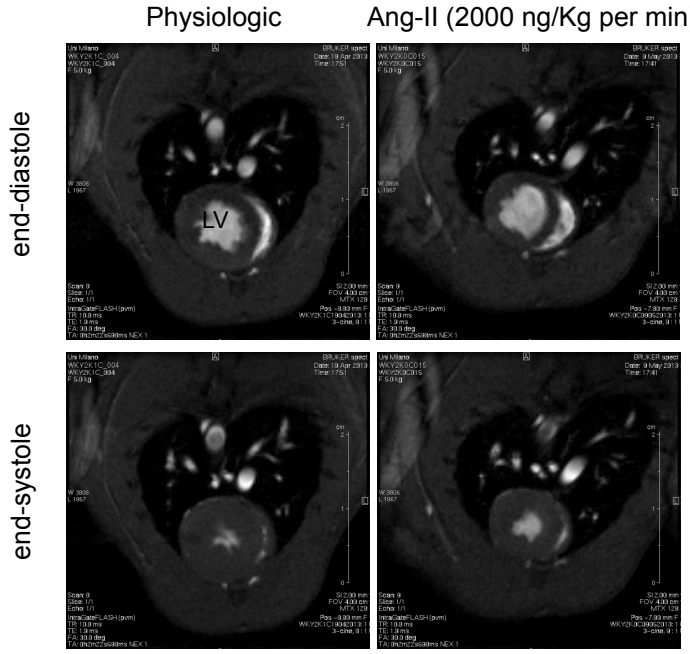

Figure 26: MRI images of short axis view in C57BL/6 mice after infusion of angiotensin II with osmotic pumps.

In figure 26 we can observe in mice treated for 14 weeks with angiotensin II a development of a dilation of left ventriculum during the end-diastole and systolic phases.

	time point	EDV (µl)	ESV (µl)	EF (%)	SV (µl)
Control	pre	60,7	18,25	70,09	42,55
	2weeks	59,85	18,05	69,7075	41,8
Ang II	pre	59,6	21,15	65,005	38,5
	2weeks	**67,1**	**29,35**	**56,175**	**37,75**

EDV: end diastolic volume
ESV: end-systolic volume
EF: ejection fraction
SV: stroke volume

Table 4: Global Left Ventricle parameters in controls and Angiotensin II infused mice.

In table 4 we observe that angiotensin infusion determines an increase of end diastolic and end systolic volume and a reduction of ejection fraction and stroke volume. These parameters indicate an induction of heart hypertrophy.

At the end of the treatment the animals were sacrified and heart tissues and plasma were collected. From the heart tissues we performed a quantitative RT-PCR analysis to see the gene expression of cardiac fetal gene, in particular ANF, BNP and skeletal muscle action (SMA), the well established surrogate markers of cardiac hypertrophy.

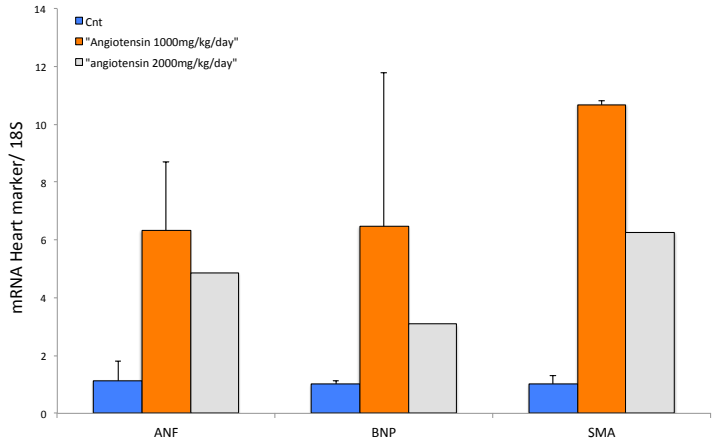

Figure 27: mRNA levels of ANF, BNP, and SMA in the heart of control and angiotensin II mice. Angiotensin II was infused in C57BL/6 mice by using osmotic pumps Alzet (mod.1004) at the rates of 1000 and 2000 mg/kg/day. After 2 weeks of treatment the mice were sacrificed, and heart phenotipic marker levels determined by RT-PCR from total RNA of cardiac tissue.

In Figure **27** we observed a very significantly increase of genes encoding for ANF BNP and SMA, the most important genes of cardiac fetal genes involved in heart hypertrophy.

In particurar we can observe how at a dose of 1000mg/kg/day of AngII there is an increasing of genes expression six times respect the control foe ANF and

BNP and ten times for SMA while at a dose of 2000mg/kg/day there is an increase of three times for ANF, two times for BNP and four times for SMA.

Evaluation of the effects of compound 4 in heart hypertrophy mouse model.

Once characterized model of cardiac hypertrophy in mice C57 BL/6, we repeated the experiment treating the mice with compound **4** for two weeks and then performed a quantitative RT-PCR to evaluate the expression of cardiac fetal genes ANF, BNP and SMA.

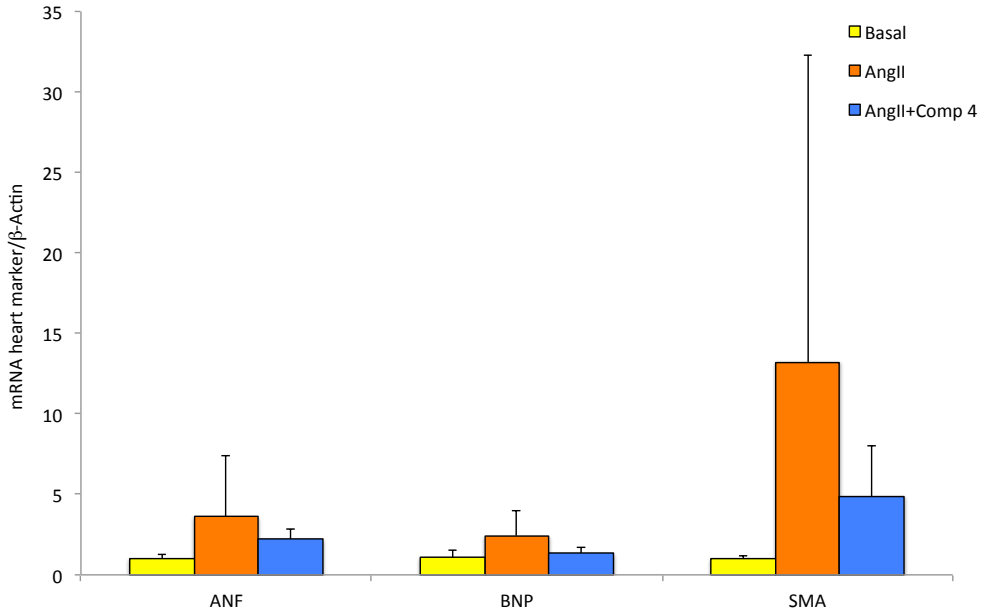

Figure 28: mRNA levels of ANF, BNP, and SMA in the hearts of angiotensin II compared to angiotensin II with compound 4 mice. Angiotensin II was infused in C57BL/6 mice by using osmotic pumps Alzet (mod.1004) at the rate of 2000 mg/kg/day. For the treated mice we administered every day 75mg/kg/day of compound **4**. After 2 weeks of treatment the mice were sacrificed, and heart phenotipic marker levels determined by RT-PCR from total RNA of cardiac tissue.

In figure **28** we observe an increase of genes encoding for ANF, BNP and SMA in mice in which it is administered Ang II, in particular we observe a significative induction of SMA. However in mice treated with compound **4** we observe a lower induction in the expression of the same genes.

These results seem to confirm that the inhibition of Rac through compound **4** may have cardioprotective effects.

Discussion

In the present study it has been utilized two different approaches to develop new Rac inhibitors: a virtual screening and a computer aided *de-novo* design of a new scaffold, starting from the previously described 3D model of the complex between Rac1 and NSC23766.

In the first approach, we started from previously identified hits[207], by using a virtual screening approach we identified a series of 3-aryl-N-aminoylsulfonylphenyl-1H-pyrazole-5-carboxamides as potent and selective Rac inhibitors. In particular, compounds **4** and **5** selectively inhibited Rac activity with IC_{50} values lower than the previously reported compounds (8.7 μM and 4.4 μM compared to 12.2 μM and 24.1 μM, respectively)[207]. The effect of the new compounds was then studied on cell adhesion, a cell-based assay directly linked to Rac activity. These set of experiments were considered more indicative of the effect of the new compounds on Rac functionality than the determination of the intracellular levels of Rac-GTP levels. The results of this analysis confirmed that all the compounds inhibited the cell adhesion with IC_{50} values similar to those observed by G-LISA assay. This observation demonstrated a direct relationship between the levels of Rac-GTP and its action on cell adhesion. In particular, compound **4** was the second most potent compound and inhibited the cell adhesion with an IC_{50} of 8.7 μM equal to that observed by G-LISA assay. Compound **4** completely inhibited lamellipodia formation in response to PDGF, a Rac1-dependent cellular effect, further confirming its inhibitory action on Rac functionality.

Other small molecules with Rac1 inhibitory activity have been described after the first discovered compound NSC23766, with some differences in their mechanisms of action. Compounds **4** and **5** appear to act, similarly to NSC23766, by interfering with the Rac1–Tiam1 interaction. The same effect was shown for NSC23766 which also interferes with the Rac1–TrioN binding, while the effect on Vav2, another GEF capable of activating Rac, was not assessed[155]. Compound **4** described in the present research program was shown to affect the Rac activity induced by three different GEFs, Tiam1, TrioN, or Vav2, and thus with a similar mechanism of action as demonstrated for compounds **4**, **5** and NSC23766. A more specific inhibitory action was then observed for the compound ITX3 which interferes with Trio without affecting the activation of Rac and RhoG by both Tiam1 and Vav2[156]. In contrast, compound EHop-016, another previously described potent Rac inhibitor, affects Vav2-mediated GDP–GTP exchange of Rac and shows a ten-fold lower affinity for Tiam1 and probably no effect on Trio[219]. While Vav2 is a GEF active on Rac1, RhoA, and Cdc42, compound EHop-016 was shown to interfere only with Rac–Vav2 interaction, a selective effect potentially responsible for the observed increased RhoA activation in cancer cells for the higher availability of Vav2[220]. Interestingly, compound **4** has shown a trend of induction of RhoA activity, although not statistically significant, suggesting a similar compensatory effect to that observed for compound EHop-016. A third chemical entity, compound EHT 1864, has been discovered to selectively

inhibit Rac without interfering with the binding between Rac and GEF[221]. Although the mechanism of action has not yet been resolved, from the obtained data a possible allosteric mechanism has been suggested for the loss of binding with nucleotide. In conclusion, through a computational approach we identified a new class of Rac inhibitors that potently and selectively reduced the intracellular levels of Rac-GTP and its activity, demonstrated by effects on the lamellipodia formation, cell adhesion, migration and a powerfull reduction of superoxide anion production (IC_{50} 1nM) in human monocytes showing how by inhibiting Rac we obtain a significantly antioxidant effect. These effects appear to be related to the inhibition of GEF-mediated GTP–GDP exchange on Rac, since compound **4** affected Rac activation induced by either Tiam1, TrioN or Vav2, implying a selective interference of Rac1–GEF interaction similar to that described for compound NSC23766.

Since this compound appeared to be suitable for investigating its effect on cardiac hypertrophy and/or atherosclerotic plaque formation in in vivo experimental models, we begun to characterize an in vivo model to cardiac hypertrophy and to evaluate the pharmacokinetic and pharmacodinamic profile of Compound **4**.

From these analysis we observed a dose-dependent effect of compound **4** on Rac1-GTP levels in the heart of mice after i.p. injection. In particular at concentration of 100mg/kg per day a very significant reduction of 95% of Rac-GTP levels was achieved, together with a Cmax at a concentration approximately equal to 5μM. However, Rac1 is expressed ubiquitously in the

body and this powerfull inhibition caused also an important adverse effect as a complete intestinal blockage, suggesting that in a future study a lower dose should be used.

Another approach used to identify new Rac inhibitors was a computer aided *de-novo* design of a new scaffold, starting from the previously described 3D model of the complex between Rac1 and NSC23766. This analysis led to the synthesis of the derivatives of arylsubstituted 2-amino-3-(phenylsulfanyl)norbornane-2-carboxylate as new potential class of Rac inhibitors. This class of compounds further improves both the potency and the effectiveness of the Rac1 inhibitory activity with IC_{50} value of 2.5 μM and a 75% reduction of Rac-GTP intracellular levels. In addition, these compounds resulted also selective for Rac1 without affecting the RhoA activity.

In the future the efficacy on heart hypertrophy of both classes of compounds will be tested by using the cardiac hypertrophy model characterized within the present work in order to establish the role of Rac on this disease and the suitability of a pharmacological intervention.

Acknowledgments

In questi tre anni di dottorato sono tante le persone che mi hanno aiutato a crescere e vivere al meglio questa mia esperienza a cui voglio dedicare questo momento importante della mia vita.

Ringrazio i miei genitori che, come al solito, mi hanno sostenuto in questa mia scelta senza mai farmi mancare tutto il loro amore, incoraggiandomi a realizzare i miei sogni, a mio fratello Guido sempre presente quando avevo bisogno di qualcuno con cui parlare o di avere una parola di conforto.
Ai miei zii e a mio cugino Edoardo che da quando sono a Milano mi hanno accolto a casa loro facendomi sentire parte della famiglia.
Grazie anche agli amici di sempre su cui posso contare per qualsiasi cosa e fare affidamento quando ho bisogno di un consiglio prezioso.

Grazie al Professor Corsini che mi ha ospitato nel suo laboratorio in questo periodo di dottorato in un'ambiente bellissimo in cui lavorare e crescere.
Alla Professoressa Barocelli che come coordinatrice del corso non mi ha mai fatto mancare il suo supporto e la sua disponibilità.

Grazie a Lorenzo, a tutte le persone del laboratorio e agli amici che ho conosciuto con cui ho condiviso tanti bellissimi momenti, senza la vostra compagnia questa avventura non sarebbe stata così speciale.

Infine un ringraziamento speciale va al mio mentore Nicola Ferri che mi ha accompagnato in questa splendida esperienza.
Grazie Nicola perchè mi hai insegnato come sia importante l'amore e l'impegno per il proprio lavoro, per la pazienza che hai avuto con me nell'insegnarmi tutto quello che so di questo splendido mestiere e nell'avermi sempre sostenuto anche di fronte ai miei errori.
Ma soprattutto grazie per la bella compagnia che avevo ogni giorno in laboratorio con cui ho condiviso tanti bei momenti.
Grazie ancora di tutto!!

References

1. Sandler, H. & Dodge, H. T. Left Ventricular Tension and Stress in Man. *Circ. Res.* **13,** 91–104 (1963).

2. Grossman, W., Jones, D. & McLaurin, L. P. Wall stress and patterns of hypertrophy in the human left ventricle. *J. Clin. Invest.* **56,** 56–64 (1975).

3. Levy, D., Garrison, R. J., Savage, D. D., Kannel, W. B. & Castelli, W. P. Prognostic implications of echocardiographically determined left ventricular mass in the Framingham Heart Study. *N. Engl. J. Med.* **322,** 1561–1566 (1990).

4. Koren, M. J., Devereux, R. B., Casale, P. N., Savage, D. D. & Laragh, J. H. Relation of left ventricular mass and geometry to morbidity and mortality in uncomplicated essential hypertension. *Ann. Intern. Med.* **114,** 345–352 (1991).

5. MEERSON, F. Z. On the mechanism of compensatory hyperfunction and insufficiency of the heart. *Cor Vasa* **3,** 161–177 (1961).

6. MEERSON, F. Z. On the mechanism of compensatory hyperfunction and insufficiency of the heart. *Cor Vasa* **3,** 161–177 (1961).

7. Armoundas, A. A., Wu, R., Juang, G., Marbán, E. & Tomaselli, G. F. Electrical and structural remodeling of the failing ventricle. *Pharmacol. Ther.* **92,** 213–230 (2001).

8. Hill, J. A. Electrical remodeling in cardiac hypertrophy. *Trends Cardiovasc. Med.* **13,** 316–322 (2003).

9. Haunstetter, A. & Izumo, S. Toward antiapoptosis as a new treatment modality. *Circ. Res.* **86,** 371–376 (2000).

10. Sergeeva, I. A. & Christoffels, V. M. Regulation of expression of atrial and brain natriuretic peptide, biomarkers for heart development and disease.

Biochim. Biophys. Acta **1832,** 2403–2413 (2013).

11. Dorn, G. W., Robbins, J. & Sugden, P. H. Phenotyping Hypertrophy Eschew Obfuscation. *Circ. Res.* **92,** 1171–1175 (2003).

12. Babior, B. M. NADPH oxidase. *Curr. Opin. Immunol.* **16,** 42–47 (2004).

13. Chabrashvili, T. *et al.* Expression and cellular localization of classic NADPH oxidase subunits in the spontaneously hypertensive rat kidney. *Hypertension* **39,** 269–274 (2002).

14. Touyz, R. M., Yao, G. & Schiffrin, E. L. c-Src induces phosphorylation and translocation of p47phox: role in superoxide generation by angiotensin II in human vascular smooth muscle cells. *Arterioscler. Thromb. Vasc. Biol.* **23,** 981–987 (2003).

15. Abo, A. *et al.* Activation of the NADPH oxidase involves the small GTP-binding protein p21rac1. *Nature* **353,** 668–670 (1991).

16. Knaus, U. G., Heyworth, P. G., Evans, T., Curnutte, J. T. & Bokoch, G. M. Regulation of phagocyte oxygen radical production by the GTP-binding protein Rac 2. *Science* **254,** 1512–1515 (1991).

17. Dorseuil, O., Reibel, L., Bokoch, G. M., Camonis, J. & Gacon, G. The Rac target NADPH oxidase p67phox interacts preferentially with Rac2 rather than Rac1. *J. Biol. Chem.* **271,** 83–88 (1996).

18. Diekmann, D., Abo, A., Johnston, C., Segal, A. W. & Hall, A. Interaction of Rac with p67phox and regulation of phagocytic NADPH oxidase activity. *Science* **265,** 531–533 (1994).

19. Heyworth, P. G., Bohl, B. P., Bokoch, G. M. & Curnutte, J. T. Rac

translocates independently of the neutrophil NADPH oxidase components p47phox and p67phox. Evidence for its interaction with flavocytochrome b558. *J. Biol. Chem.* **269,** 30749–30752 (1994).

20. Kreck, M. L., Freeman, J. L., Abo, A. & Lambeth, J. D. Membrane association of Rac is required for high activity of the respiratory burst oxidase. *Biochemistry (Mosc.)* **35,** 15683–15692 (1996).

21. Koga, H. *et al.* Tetratricopeptide repeat (TPR) motifs of p67(phox) participate in interaction with the small GTPase Rac and activation of the phagocyte NADPH oxidase. *J. Biol. Chem.* **274,** 25051–25060 (1999).

22. Diebold, B. A. & Bokoch, G. M. Molecular basis for Rac2 regulation of phagocyte NADPH oxidase. *Nat. Immunol.* **2,** 211–215 (2001).

23. Sun, M. *et al.* Rac1 is a possible link between obesity and oxidative stress in Chinese overweight adolescents. *Obes. Silver Spring Md* **20,** 2233–2240 (2012).

24. Huang, P. L. Unraveling the links between diabetes, obesity, and cardiovascular disease. *Circ. Res.* **96,** 1129–1131 (2005).

25. Beckman, J. S. & Koppenol, W. H. Nitric oxide, superoxide, and peroxynitrite: the good, the bad, and ugly. *Am. J. Physiol.* **271,** C1424–1437 (1996).

26. DeLeo, F. R. & Quinn, M. T. Assembly of the phagocyte NADPH oxidase: molecular interaction of oxidase proteins. *J. Leukoc. Biol.* **60,** 677–691 (1996).

27. Babior, B. M., Lambeth, J. D. & Nauseef, W. The neutrophil NADPH oxidase. *Arch. Biochem. Biophys.* **397,** 342–344 (2002).

28. Nishikimi, T., Maeda, N. & Matsuoka, H. The role of natriuretic peptides in cardioprotection. *Cardiovasc. Res.* **69,** 318–328 (2006).

29. Bruneau, B. G. *et al.* A Murine Model of Holt-Oram Syndrome Defines Roles of the T-Box Transcription Factor Tbx5 in Cardiogenesis and Disease. *Cell* **106,** 709–721 (2001).

30. De Bold, A. J., Borenstein, H. B., Veress, A. T. & Sonnenberg, H. A rapid and potent natriuretic response to intravenous injection of atrial myocardial extract in rats. *Life Sci.* **28,** 89–94 (1981).

31. Bianchi, C. *et al.* Radioautographic localization of125I-atrial natriuretic fator (ANF) in rat tissues. *Histochemistry* **82,** 441–452 (1985).

32. Jacobowitz, D. M., Skofitsch, G., Keiser, H. R., Eskay, R. L. & Zamir, N. Evidence for the Existence of Atrial Natriuretic Factor-Containing Neurons in the Rat Brain. *Neuroendocrinology* **40,** 92–94 (1985).

33. Tanaka, I., Misono, K. S. & Inagami, T. Atrial natriuretic factor in rat hypothalamus, atria and plasma: Determination by specific radioimmunoassay. *Biochem. Biophys. Res. Commun.* **124,** 663–668 (1984).

34. Ueda, S. *et al.* Identification of alpha atrial natriuretic peptide [4–28] and [5–28] in porcine brain. *Biochem. Biophys. Res. Commun.* **149,** 1055–1062 (1987).

35. Sudoh, T., Kangawa, K., Minamino, N. & Matsuo, H. A new natriuretic peptide in porcine brain. *Nature* **332,** 78–81 (1988).

36. Gutkowska, J., Antunes-Rodrigues, J. & Mccann, S. M. Atrial natriuretic peptide in brain and pituitary gland. *Physiol. Rev.* **77,** 465–515 (1997).

37. Thibault, G., Charbonneau, C., Bilodeau, J., Schiffrin, E. L. & Garcia, R. Rat brain natriuretic peptide is localized in atrial granules and released into the circulation. *Am. J. Physiol. - Regul. Integr. Comp. Physiol.* **263,** R301–R309 (1992).

38. Shimoike, H., Iwai, N. & Kinoshita, M. Differential Regulation of Natriuretic Peptide Genes in Infarcted Rat Hearts. *Clin. Exp. Pharmacol. Physiol.* **24,** 23–30 (1997).

39. Hori, Y. *et al.* Acute cardiac volume load-related changes in plasma atrial natriuretic peptide and N-terminal pro-B-type natriuretic peptide concentrations in healthy dogs. *Vet. J.* **185,** 317–321 (2010).

40. Mäntymaa, P., Vuolteenaho, O., Marttila, M. & Ruskoaho, H. Atrial stretch induces rapid increase in brain natriuretic peptide but not in atrial natriuretic peptide gene expression in vitro. *Endocrinology* **133,** 1470–1473 (1993).

41. Bruneau, B. G. & Bold, A. J. D. Selective changes in natriuretic peptide and early response gene expression in isolated rat atria following stimulation by stretch or endothelin-1. *Cardiovasc. Res.* **28,** 1519–1525 (1994).

42. Kinnunen, P., Vuolteenaho, O. & Ruskoaho, H. Mechanisms of atrial and brain natriuretic peptide release from rat ventricular myocardium: effect of stretching. *Endocrinology* **132,** 1961–1970 (1993).

43. Ruskoaho, H. *et al.* Regulation of ventricular atrial natriuretic peptide release in hypertrophied rat myocardium. Effects of exercise. *Circulation* **80,** 390–400 (1989).

44. Agnoletti, G. *et al.* Effect of congestive heart failure on rate of atrial

natriuretic factor release in response to stretch and isoprenaline. *Cardiovasc. Res.* **24,** 938–945 (1990).

45. Shimoike, H., Iwai, N. & Kinoshita, M. Differential Regulation of Natriuretic Peptide Genes in Infarcted Rat Hearts. *Clin. Exp. Pharmacol. Physiol.* **24,** 23–30 (1997).

46. Shimoike, H., Iwai, N. & Kinoshita, M. Differential Regulation of Natriuretic Peptide Genes in Infarcted Rat Hearts. *Clin. Exp. Pharmacol. Physiol.* **24,** 23–30 (1997).

47. Lear, W. & Boer, P. H. Rapid activation of the type B versus type A natriuretic factor gene by aortocaval shunt induced cardiac volume overload. *Cardiovasc. Res.* **29,** 676–681 (1995).

48. Hama, N. *et al.* Rapid Ventricular Induction of Brain Natriuretic Peptide Gene Expression in Experimental Acute Myocardial Infarction. *Circulation* **92,** 1558–1564 (1995).

49. Lear, W. & Boer, P. H. Rapid activation of the type B versus type A natriuretic factor gene by aortocaval shunt induced cardiac volume overload. *Cardiovasc. Res.* **29,** 676–681 (1995).

50. Wolf, K. *et al.* Different regulation of left ventricular ANP, BNP and adrenomedullin mRNA in the two-kidney, one-clip model of renovascular hypertension. *Pflüg. Arch.* **442,** 212–217 (2001).

51. Lear, W. & Boer, P. H. Rapid activation of the type B versus type A natriuretic factor gene by aortocaval shunt induced cardiac volume overload. *Cardiovasc. Res.* **29,** 676–681 (1995).

52. Mäntymaa, P., Vuolteenaho, O., Marttila, M. & Ruskoaho, H. Atrial stretch induces rapid increase in brain natriuretic peptide but not in atrial natriuretic peptide gene expression in vitro. *Endocrinology* **133,** 1470–1473 (1993).

53. Pikkarainen, S. *et al.* GATA-4 Is a Nuclear Mediator of Mechanical Stretch-activated Hypertrophic Program. *J. Biol. Chem.* **278,** 23807–23816 (2003).

54. Kerkelä, R. *et al.* Key roles of endothelin-1 and p38 MAPK in the regulation of atrial stretch response. *Am. J. Physiol. - Regul. Integr. Comp. Physiol.* **300,** R140–R149 (2011).

55. Kerkelä, R. *et al.* Key roles of endothelin-1 and p38 MAPK in the regulation of atrial stretch response. *Am. J. Physiol. Regul. Integr. Comp. Physiol.* **300,** R140–149 (2011).

56. Aikawa, R. *et al.* Integrins play a critical role in mechanical stress-induced p38 MAPK activation. *Hypertension* **39,** 233–238 (2002).

57. Liang, F., Lu, S. & Gardner, D. G. Endothelin-Dependent and -Independent Components of Strain-Activated Brain Natriuretic Peptide Gene Transcription Require Extracellular Signal Regulated Kinase and p38 Mitogen-Activated Protein Kinase. *Hypertension* **35,** 188–192 (2000).

58. Liang, F. & Gardner, D. G. Autocrine/Paracrine Determinants of Strain-activated Brain Natriuretic Peptide Gene Expression in Cultured Cardiac Myocytes. *J. Biol. Chem.* **273,** 14612–14619 (1998).

59. Rosenkranz, S. TGF-β1 and angiotensin networking in cardiac remodeling. *Cardiovasc. Res.* **63,** 423–432 (2004).

60. Majalahti, T. *et al.* Cardiac BNP gene activation by angiotensin II in vivo. *Mol. Cell. Endocrinol.* **273,** 59–67 (2007).

61. Etienne-Manneville, S. & Hall, A. Rho GTPases in cell biology. *Nature* **420,** 629–635 (2002).

62. Seabra, M. C. Membrane association and targeting of prenylated Ras-like GTPases. *Cell. Signal.* **10,** 167–172 (1998).

63. Hall, A. Rho GTPases and the actin cytoskeleton. *Science* **279,** 509–514 (1998).

64. Heo, W. D. & Meyer, T. Switch-of-function mutants based on morphology classification of Ras superfamily small GTPases. *Cell* **113,** 315–328 (2003).

65. Sugden, P. H. & Clerk, A. Activation of the small GTP-binding protein Ras in the heart by hypertrophic agonists. *Trends Cardiovasc. Med.* **10,** 1–8 (2000).

66. Ridley, A. J. & Hall, A. The small GTP-binding protein rho regulates the assembly of focal adhesions and actin stress fibers in response to growth factors. *Cell* **70,** 389–399 (1992).

67. Riento, K. & Ridley, A. J. Rocks: multifunctional kinases in cell behaviour. *Nat. Rev. Mol. Cell Biol.* **4,** 446–456 (2003).

68. Noda, M. *et al.* Involvement of rho in GTP gamma S-induced enhancement of phosphorylation of 20 kDa myosin light chain in vascular smooth muscle cells: inhibition of phosphatase activity. *FEBS Lett.* **367,** 246–250 (1995).

69. Kimura, K. *et al.* Regulation of myosin phosphatase by Rho and Rho-associated kinase (Rho-kinase). *Science* **273,** 245–248 (1996).

70. Kureishi, Y. *et al.* Rho-associated kinase directly induces smooth muscle contraction through myosin light chain phosphorylation. *J. Biol. Chem.* **272,** 12257–12260 (1997).

71. Seasholtz, T. M. *et al.* Increased expression and activity of RhoA are associated with increased DNA synthesis and reduced p27(Kip1) expression in the vasculature of hypertensive rats. *Circ. Res.* **89,** 488–495 (2001).

72. Moriki, N. *et al.* RhoA activation in vascular smooth muscle cells from stroke-prone spontaneously hypertensive rats. *Hypertens. Res. Off. J. Jpn. Soc. Hypertens.* **27,** 263–270 (2004).

73. Seko, T. *et al.* Activation of RhoA and inhibition of myosin phosphatase as important components in hypertension in vascular smooth muscle. *Circ. Res.* **92,** 411–418 (2003).

74. Sah, V. P. *et al.* Cardiac-specific overexpression of RhoA results in sinus and atrioventricular nodal dysfunction and contractile failure. *J. Clin. Invest.* **103,** 1627–1634 (1999).

75. Rikitake, Y. *et al.* Decreased perivascular fibrosis but not cardiac hypertrophy in ROCK1+/- haploinsufficient mice. *Circulation* **112,** 2959–2965 (2005).

76. Porter, K. E., Turner, N. A., O'Regan, D. J., Balmforth, A. J. & Ball, S. G. Simvastatin reduces human atrial myofibroblast proliferation independently of cholesterol lowering via inhibition of RhoA. *Cardiovasc. Res.* **61,** 745–755 (2004).

77. Takenawa, T. & Miki, H. WASP and WAVE family proteins: key molecules

for rapid rearrangement of cortical actin filaments and cell movement. *J. Cell Sci.* **114,** 1801–1809 (2001).

78. Teramoto, H. *et al.* Signaling from the small GTP-binding proteins Rac1 and Cdc42 to the c-Jun N-terminal kinase/stress-activated protein kinase pathway. A role for mixed lineage kinase 3/protein-tyrosine kinase 1, a novel member of the mixed lineage kinase family. *J. Biol. Chem.* **271,** 27225–27228 (1996).

79. Takenawa, T. & Miki, H. WASP and WAVE family proteins: key molecules for rapid rearrangement of cortical actin filaments and cell movement. *J. Cell Sci.* **114,** 1801–1809 (2001).

80. Gregg, D., Rauscher, F. M. & Goldschmidt-Clermont, P. J. Rac regulates cardiovascular superoxide through diverse molecular interactions: more than a binary GTP switch. *Am. J. Physiol. Cell Physiol.* **285,** C723–734 (2003).

81. Marinissen, M. J., Chiariello, M. & Gutkind, J. S. Regulation of gene expression by the small GTPase Rho through the ERK6 (p38 gamma) MAP kinase pathway. *Genes Dev.* **15,** 535–553 (2001).

82. Marinissen, M. J. *et al.* The small GTP-binding protein RhoA regulates c-jun by a ROCK-JNK signaling axis. *Mol. Cell* **14,** 29–41 (2004).

83. Charron, F. *et al.* Tissue-specific GATA factors are transcriptional effectors of the small GTPase RhoA. *Genes Dev.* **15,** 2702–2719 (2001).

84. Anwar, K. N., Fazal, F., Malik, A. B. & Rahman, A. RhoA/Rho-associated kinase pathway selectively regulates thrombin-induced intercellular adhesion molecule-1 expression in endothelial cells via activation of I kappa B kinase

beta and phosphorylation of RelA/p65. *J. Immunol. Baltim. Md 1950* **173,** 6965–6972 (2004).

85. Benitah, S. A., Valerón, P. F. & Lacal, J. C. ROCK and nuclear factor-kappaB-dependent activation of cyclooxygenase-2 by Rho GTPases: effects on tumor growth and therapeutic consequences. *Mol. Biol. Cell* **14,** 3041–3054 (2003).

86. Takano, H. *et al.* The Rho family G proteins play a critical role in muscle differentiation. *Mol. Cell. Biol.* **18,** 1580–1589 (1998).

87. Chang, S., Bezprozvannaya, S., Li, S. & Olson, E. N. An expression screen reveals modulators of class II histone deacetylase phosphorylation. *Proc. Natl. Acad. Sci. U. S. A.* **102,** 8120–8125 (2005).

88. Pracyk, J. B. *et al.* A requirement for the rac1 GTPase in the signal transduction pathway leading to cardiac myocyte hypertrophy. *J. Clin. Invest.* **102,** 929–937 (1998).

89. Clerk, A. *et al.* Regulation of mitogen-activated protein kinases in cardiac myocytes through the small G protein Rac1. *Mol. Cell. Biol.* **21,** 1173–1184 (2001).

90. Aikawa, R. *et al.* Reactive oxygen species in mechanical stress-induced cardiac hypertrophy. *Biochem. Biophys. Res. Commun.* **289,** 901–907 (2001).

91. Buscemi, N., Foster, D. B., Neverova, I. & Van Eyk, J. E. p21-activated kinase increases the calcium sensitivity of rat triton-skinned cardiac muscle fiber bundles via a mechanism potentially involving novel phosphorylation of troponin I. *Circ. Res.* **91,** 509–516 (2002).

92. Elnakish, M. T. *et al.* Cardiac remodeling caused by transgenic overexpression of a corn Rac gene. *Am. J. Physiol. Heart Circ. Physiol.* **301,** H868–880 (2011).

93. Belch, J. J., Bridges, A. B., Scott, N. & Chopra, M. Oxygen free radicals and congestive heart failure. *Br. Heart J.* **65,** 245–248 (1991).

94. Mallat, Z. *et al.* Elevated levels of 8-iso-prostaglandin F2alpha in pericardial fluid of patients with heart failure: a potential role for in vivo oxidant stress in ventricular dilatation and progression to heart failure. *Circulation* **97,** 1536–1539 (1998).

95. Aikawa, R. *et al.* Insulin prevents cardiomyocytes from oxidative stress-induced apoptosis through activation of PI3 kinase/Akt. *Circulation* **102,** 2873–2879 (2000).

96. MacCarthy, P. A. *et al.* Impaired endothelial regulation of ventricular relaxation in cardiac hypertrophy: role of reactive oxygen species and NADPH oxidase. *Circulation* **104,** 2967–2974 (2001).

97. Pracyk, J. B. *et al.* A requirement for the rac1 GTPase in the signal transduction pathway leading to cardiac myocyte hypertrophy. *J. Clin. Invest.* **102,** 929–937 (1998).

98. Takemoto, M. *et al.* Statins as antioxidant therapy for preventing cardiac myocyte hypertrophy. *J. Clin. Invest.* **108,** 1429–1437 (2001).

99. Laufs, U. *et al.* Impact of HMG CoA reductase inhibition on small GTPases in the heart. *Cardiovasc. Res.* **53,** 911–920 (2002).

100. Takemoto, M. *et al.* Statins as antioxidant therapy for preventing cardiac

myocyte hypertrophy. *J. Clin. Invest.* **108,** 1429–1437 (2001).

101. Wassmann, S. *et al.* Inhibition of geranylgeranylation reduces angiotensin II-mediated free radical production in vascular smooth muscle cells: involvement of angiotensin AT1 receptor expression and Rac1 GTPase. *Mol. Pharmacol.* **59,** 646–654 (2001).

102. Maack, C. *et al.* Oxygen free radical release in human failing myocardium is associated with increased activity of rac1-GTPase and represents a target for statin treatment. *Circulation* **108,** 1567–1574 (2003).

103. Ross, R. Atherosclerosis is an inflammatory disease. *Am. Heart J.* **138,** S419–420 (1999).

104. Glagov, S., Weisenberg, E., Zarins, C. K., Stankunavicius, R. & Kolettis, G. J. Compensatory enlargement of human atherosclerotic coronary arteries. *N. Engl. J. Med.* **316,** 1371–1375 (1987).

105. Small, D. M. George Lyman Duff memorial lecture. Progression and regression of atherosclerotic lesions. Insights from lipid physical biochemistry. *Arterioscler. Dallas Tex* **8,** 103–129 (1988).

106. Wilcox, J. N., Smith, K. M., Schwartz, S. M. & Gordon, D. Localization of tissue factor in the normal vessel wall and in the atherosclerotic plaque. *Proc. Natl. Acad. Sci. U. S. A.* **86,** 2839–2843 (1989).

107. Loree, H. M., Kamm, R. D., Stringfellow, R. G. & Lee, R. T. Effects of fibrous cap thickness on peak circumferential stress in model atherosclerotic vessels. *Circ. Res.* **71,** 850–858 (1992).

108. Loree, H. M., Kamm, R. D., Stringfellow, R. G. & Lee, R. T. Effects of fibrous

cap thickness on peak circumferential stress in model atherosclerotic vessels. *Circ. Res.* **71,** 850–858 (1992).

109. Burleigh, M. C. *et al.* Collagen types I and III, collagen content, GAGs and mechanical strength of human atherosclerotic plaque caps: span-wise variations. *Atherosclerosis* **96,** 71–81 (1992).

110. Ross, R. & Glomset, J. A. Atherosclerosis and the arterial smooth muscle cell: Proliferation of smooth muscle is a key event in the genesis of the lesions of atherosclerosis. *Science* **180,** 1332–1339 (1973).

111. Ridley, A. J. *et al.* Cell migration: integrating signals from front to back. *Science* **302,** 1704–1709 (2003).

112. Raines, E. W. & Ferri, N. Thematic review series: The immune system and atherogenesis. Cytokines affecting endothelial and smooth muscle cells in vascular disease. *J. Lipid Res.* **46,** 1081–1092 (2005).

113. Doanes, A. M., Irani, K., Goldschmidt-Clermont, P. J. & Finkel, T. A requirement for rac1 in the PDGF-stimulated migration of fibroblasts and vascular smooth cells. *Biochem. Mol. Biol. Int.* **45,** 279–287 (1998).

114. Vega, F. M., Colomba, A., Reymond, N., Thomas, M. & Ridley, A. J. RhoB regulates cell migration through altered focal adhesion dynamics. *Open Biol.* **2,** 120076 (2012).

115. Cheng, Z. *et al.* Focal adhesion kinase regulates smooth muscle cell recruitment to the developing vasculature. *Arterioscler. Thromb. Vasc. Biol.* **31,** 2193–2202 (2011).

116. Weber, D. S. *et al.* Phosphoinositide-dependent kinase 1 and p21-

activated protein kinase mediate reactive oxygen species-dependent regulation of platelet-derived growth factor-induced smooth muscle cell migration. *Circ. Res.* **94,** 1219–1226 (2004).

117. Lee, M. Y. & Griendling, K. K. Redox signaling, vascular function, and hypertension. *Antioxid. Redox Signal.* **10,** 1045–1059 (2008).

118. Schröder, K. *et al.* Nox1 mediates basic fibroblast growth factor-induced migration of vascular smooth muscle cells. *Arterioscler. Thromb. Vasc. Biol.* **27,** 1736–1743 (2007).

119. Rus, H. G., Niculescu, F. & Vlaicu, R. Tumor necrosis factor-alpha in human arterial wall with atherosclerosis. *Atherosclerosis* **89,** 247–254 (1991).

120. Clausell, N., Molossi, S., Sett, S. & Rabinovitch, M. In vivo blockade of tumor necrosis factor-alpha in cholesterol-fed rabbits after cardiac transplant inhibits acute coronary artery neointimal formation. *Circulation* **89,** 2768–2779 (1994).

121. Rectenwald, J. E., Moldawer, L. L., Huber, T. S., Seeger, J. M. & Ozaki, C. K. Direct evidence for cytokine involvement in neointimal hyperplasia. *Circulation* **102,** 1697–1702 (2000).

122. Ono, H. *et al.* cAMP-response element-binding protein mediates tumor necrosis factor-alpha-induced vascular smooth muscle cell migration. *Arterioscler. Thromb. Vasc. Biol.* **24,** 1634–1639 (2004).

123. Qu, M.-J., Liu, B., Qi, Y.-X. & Jiang, Z.-L. Role of Rac and Rho-GDI alpha in the frequency-dependent expression of h1-calponin in vascular smooth muscle cells under cyclic mechanical strain. *Ann. Biomed. Eng.* **36,** 1481–1488 (2008).

124. Ferri, N. *et al.* Simvastatin reduces MMP1 expression in human smooth muscle cells cultured on polymerized collagen by inhibiting Rac1 activation. *Arterioscler. Thromb. Vasc. Biol.* **27,** 1043–1049 (2007).

125. Bond, M., Wu, Y.-J., Sala-Newby, G. B. & Newby, A. C. Rho GTPase, Rac1, regulates Skp2 levels, vascular smooth muscle cell proliferation, and intima formation in vitro and in vivo. *Cardiovasc. Res.* **80,** 290–298 (2008).

126. Libby, P. Inflammation in atherosclerosis. *Arterioscler. Thromb. Vasc. Biol.* **32,** 2045–2051 (2012).

127. Kraynov, V. S. *et al.* Localized Rac activation dynamics visualized in living cells. *Science* **290,** 333–337 (2000).

128. Chigaev, A. *et al.* Alpha4beta1 integrin affinity changes govern cell adhesion. *J. Biol. Chem.* **278,** 38174–38182 (2003).

129. Jones, G. E., Allen, W. E. & Ridley, A. J. The Rho GTPases in macrophage motility and chemotaxis. *Cell Adhes. Commun.* **6,** 237–245 (1998).

130. Allen, W. E., Jones, G. E., Pollard, J. W. & Ridley, A. J. Rho, Rac and Cdc42 regulate actin organization and cell adhesion in macrophages. *J. Cell Sci.* **110 (Pt 6),** 707–720 (1997).

131. Tzima, E. *et al.* Activation of Rac1 by shear stress in endothelial cells mediates both cytoskeletal reorganization and effects on gene expression. *EMBO J.* **21,** 6791–6800 (2002).

132. Wojciak-Stothard, B. & Ridley, A. J. Shear stress-induced endothelial cell polarization is mediated by Rho and Rac but not Cdc42 or PI 3-kinases. *J. Cell Biol.* **161,** 429–439 (2003).

133. Orr, A. W., Hahn, C., Blackman, B. R. & Schwartz, M. A. p21-activated kinase signaling regulates oxidant-dependent NF-kappa B activation by flow. *Circ. Res.* **103,** 671–679 (2008).

134. Orr, A. W. *et al.* Matrix-specific p21-activated kinase activation regulates vascular permeability in atherogenesis. *J. Cell Biol.* **176,** 719–727 (2007).

135. Moldovan, L., Mythreye, K., Goldschmidt-Clermont, P. J. & Satterwhite, L. L. Reactive oxygen species in vascular endothelial cell motility. Roles of NAD(P)H oxidase and Rac1. *Cardiovasc. Res.* **71,** 236–246 (2006).

136. Noritake, J. *et al.* Positive role of IQGAP1, an effector of Rac1, in actin-meshwork formation at sites of cell-cell contact. *Mol. Biol. Cell* **15,** 1065–1076 (2004).

137. Stockton, R. A., Schaefer, E. & Schwartz, M. A. p21-activated kinase regulates endothelial permeability through modulation of contractility. *J. Biol. Chem.* **279,** 46621–46630 (2004).

138. Sakata, Y. *et al.* Transcription factor CHF1/Hey2 regulates neointimal formation in vivo and vascular smooth muscle proliferation and migration in vitro. *Arterioscler. Thromb. Vasc. Biol.* **24,** 2069–2074 (2004).

139. Ashino, T., Yamamoto, M., Yoshida, T. & Numazawa, S. Redox-sensitive transcription factor Nrf2 regulates vascular smooth muscle cell migration and neointimal hyperplasia. *Arterioscler. Thromb. Vasc. Biol.* **33,** 760–768 (2013).

140. Lee, H. M. *et al.* Gene transfer of redox factor-1 inhibits neointimal formation: involvement of platelet-derived growth factor-beta receptor signaling via the inhibition of the reactive oxygen species-mediated Syk

pathway. *Circ. Res.* **104,** 219–227, 5p following 227 (2009).

141. Barry-Lane, P. A. *et al.* p47phox is required for atherosclerotic lesion progression in ApoE(-/-) mice. *J. Clin. Invest.* **108,** 1513–1522 (2001).

142. Chen, Z. *et al.* Decreased neointimal formation in Nox2-deficient mice reveals a direct role for NADPH oxidase in the response to arterial injury. *Proc. Natl. Acad. Sci. U. S. A.* **101,** 13014–13019 (2004).

143. Levy, D., Garrison, R. J., Savage, D. D., Kannel, W. B. & Castelli, W. P. Prognostic implications of echocardiographically determined left ventricular mass in the Framingham Heart Study. *N. Engl. J. Med.* **322,** 1561–1566 (1990).

144. Sawada, N., Salomone, S., Kim, H.-H., Kwiatkowski, D. J. & Liao, J. K. Regulation of endothelial nitric oxide synthase and postnatal angiogenesis by Rac1. *Circ. Res.* **103,** 360–368 (2008).

145. Sakata, Y. *et al.* Ventricular septal defect and cardiomyopathy in mice lacking the transcription factor CHF1/Hey2. *Proc. Natl. Acad. Sci. U. S. A.* **99,** 16197–16202 (2002).

146. Wu, J.-H. *et al.* Kalirin promotes neointimal hyperplasia by activating Rac in smooth muscle cells. *Arterioscler. Thromb. Vasc. Biol.* **33,** 702–708 (2013).

147. Bellosta, S., Ferri, N., Bernini, F., Paoletti, R. & Corsini, A. Non-lipid-related effects of statins. *Ann. Med.* **32,** 164–176 (2000).

148. Ferri, N. *et al.* Effect of S(-) perillic acid on protein prenylation and arterial smooth muscle cell proliferation. *Biochem. Pharmacol.* **62,** 1637–1645 (2001).

149. Ferri, N. *et al.* Ajoene, a garlic compound, inhibits protein prenylation

and arterial smooth muscle cell proliferation. *Br. J. Pharmacol.* **138,** 811–818 (2003).

150. Zhou, Q. & Liao, J. K. Pleiotropic effects of statins. - Basic research and clinical perspectives -. *Circ. J. Off. J. Jpn. Circ. Soc.* **74,** 818–826 (2010).

151. Cholesterol Treatment Trialists' (CTT) Collaborators *et al.* The effects of lowering LDL cholesterol with statin therapy in people at low risk of vascular disease: meta-analysis of individual data from 27 randomised trials. *Lancet* **380,** 581–590 (2012).

152. Cicha, I., Schneiderhan-Marra, N., Yilmaz, A., Garlichs, C. D. & Goppelt-Struebe, M. Monitoring the cellular effects of HMG-CoA reductase inhibitors in vitro and ex vivo. *Arterioscler. Thromb. Vasc. Biol.* **24,** 2046–2050 (2004).

153. Worthylake, D. K., Rossman, K. L. & Sondek, J. Crystal structure of Rac1 in complex with the guanine nucleotide exchange region of Tiam1. *Nature* **408,** 682–688 (2000).

154. Gao, Y., Xing, J., Streuli, M., Leto, T. L. & Zheng, Y. Trp(56) of rac1 specifies interaction with a subset of guanine nucleotide exchange factors. *J. Biol. Chem.* **276,** 47530–47541 (2001).

155. Gao, Y., Dickerson, J. B., Guo, F., Zheng, J. & Zheng, Y. Rational design and characterization of a Rac GTPase-specific small molecule inhibitor. *Proc. Natl. Acad. Sci. U. S. A.* **101,** 7618–7623 (2004).

156. Bouquier, N. *et al.* A cell active chemical GEF inhibitor selectively targets the Trio/RhoG/Rac1 signaling pathway. *Chem. Biol.* **16,** 657–666 (2009).

157. Blangy, A. *et al.* Identification of TRIO-GEFD1 chemical inhibitors using

the yeast exchange assay. *Biol. Cell Auspices Eur. Cell Biol. Organ.* **98,** 511–522 (2006).

158. Montalvo-Ortiz, B. L. *et al.* Characterization of EHop-016, novel small molecule inhibitor of Rac GTPase. *J. Biol. Chem.* **287,** 13228–13238 (2012).

159. Montalvo-Ortiz, B. L. *et al.* Characterization of EHop-016, novel small molecule inhibitor of Rac GTPase. *J. Biol. Chem.* **287,** 13228–13238 (2012).

160. Huh, J. Y. *et al.* 8-Hydroxy-2-deoxyguanosine prevents plaque formation and inhibits vascular smooth muscle cell activation through Rac1 inactivation. *Free Radic. Biol. Med.* **53,** 109–121 (2012).

161. Lee, S.-H. *et al.* Inhibition of Rac and Rac-linked functions by 8-oxo-2'-deoxyguanosine in murine macrophages. *Free Radic. Res.* **43,** 78–84 (2009).

162. Seshiah, P. N. *et al.* Angiotensin II stimulation of NAD(P)H oxidase activity: upstream mediators. *Circ. Res.* **91,** 406–413 (2002).

163. Kong, G., Lee, S. & Kim, K. S. Inhibition of rac1 reduces PDGF-induced reactive oxygen species and proliferation in vascular smooth muscle cells. *J. Korean Med. Sci.* **16,** 712–718 (2001).

164. Cancelas, J. A. *et al.* Rac GTPases differentially integrate signals regulating hematopoietic stem cell localization. *Nat. Med.* **11,** 886–891 (2005).

165. Lee, S.-H. *et al.* Inhibition of Rac and Rac-linked functions by 8-oxo-2'-deoxyguanosine in murine macrophages. *Free Radic. Res.* **43,** 78–84 (2009).

166. ZBINDEN, G. & BAGDON, R. E. ISOPROTERENOL-INDUCED HEART NECROSIS, AN EXPERIMENTAL MODEL FOR THE STUDY OF ANGINA PECTORIS AND MYOCARDIAL INFARCT. *Rev. Can. Biol. Éditée Par Univ. Montr.*

22, 257–263 (1963).

167. Adler, N., Camin, L. L. & Shulkin, P. Rat model for acute myocardial infarction: application to technetium-labeled glucoheptonate, tetracycline, and polyphosphate. *J. Nucl. Med. Off. Publ. Soc. Nucl. Med.* **17,** 203–207 (1976).

168. Pfeffer, M. A. *et al.* Myocardial infarct size and ventricular function in rats. *Circ. Res.* **44,** 503–512 (1979).

169. Fletcher, P. J., Pfeffer, J. M., Pfeffer, M. A. & Braunwald, E. Left ventricular diastolic pressure-volume relations in rats with healed myocardial infarction. Effects on systolic function. *Circ. Res.* **49,** 618–626 (1981).

170. Pfeffer, J. M., Pfeffer, M. A. & Braunwald, E. Influence of chronic captopril therapy on the infarcted left ventricle of the rat. *Circ. Res.* **57,** 84–95 (1985).

171. Pfeffer, M. A., Pfeffer, J. M., Steinberg, C. & Finn, P. Survival after an experimental myocardial infarction: beneficial effects of long-term therapy with captopril. *Circulation* **72,** 406–412 (1985).

172. Pfeffer, M. A. *et al.* Effect of captopril on mortality and morbidity in patients with left ventricular dysfunction after myocardial infarction. Results of the survival and ventricular enlargement trial. The SAVE Investigators. *N. Engl. J. Med.* **327,** 669–677 (1992).

173. Sutton, M. S. J. *et al.* Quantitative two-dimensional echocardiographic measurements are major predictors of adverse cardiovascular events after acute myocardial infarction. The protective effects of captopril. *Circulation* **89,** 68–75 (1994).

174. Smits, J. F., van Krimpen, C., Schoemaker, R. G., Cleutjens, J. P. & Daemen,

M. J. Angiotensin II receptor blockade after myocardial infarction in rats: effects on hemodynamics, myocardial DNA synthesis, and interstitial collagen content. *J. Cardiovasc. Pharmacol.* **20,** 772–778 (1992).

175. Hayashi, N., Fujimura, Y., Yamamoto, S., Kometani, M. & Nakao, K. Pharmacological profile of valsartan, a non-peptide angiotensin II type 1 receptor antagonist. 4th communication: improvement of heart failure of rats with myocardial infarction by valasartan. *Arzneimittelforschung.* **47,** 625–629 (1997).

176. Litwin, S. E. *et al.* Serial echocardiographic-Doppler assessment of left ventricular geometry and function in rats with pressure-overload hypertrophy. Chronic angiotensin-converting enzyme inhibition attenuates the transition to heart failure. *Circulation* **91,** 2642–2654 (1995).

177. Miyamoto, M. I. *et al.* Adenoviral gene transfer of SERCA2a improves left-ventricular function in aortic-banded rats in transition to heart failure. *Proc. Natl. Acad. Sci. U. S. A.* **97,** 793–798 (2000).

178. Del Monte, F. *et al.* Improvement in survival and cardiac metabolism after gene transfer of sarcoplasmic reticulum Ca(2+)-ATPase in a rat model of heart failure. *Circulation* **104,** 1424–1429 (2001).

179. Hajjar, R. J. *et al.* Design of a phase 1/2 trial of intracoronary administration of AAV1/SERCA2a in patients with heart failure. *J. Card. Fail.* **14,** 355–367 (2008).

180. Inoko, M., Kihara, Y., Morii, I., Fujiwara, H. & Sasayama, S. Transition from compensatory hypertrophy to dilated, failing left ventricles in Dahl salt-

sensitive rats. *Am. J. Physiol.* **267,** H2471–2482 (1994).

181. Patten, R. D. & Hall-Porter, M. R. Small Animal Models of Heart Failure: Development of Novel Therapies, Past and Present. *Circ. Heart Fail.* **2,** 138–144 (2009).

182. Heyen, J. R. R. *et al.* Structural, functional, and molecular characterization of the SHHF model of heart failure. *Am. J. Physiol. Heart Circ. Physiol.* **283,** H1775–1784 (2002).

183. Luo, J., Fujikura, K., Homma, S. & Konofagou, E. E. Myocardial elastography at both high temporal and spatial resolution for the detection of infarcts. *Ultrasound Med. Biol.* **33,** 1206–1223 (2007).

184. Georgakopoulos, D. *et al.* In vivo murine left ventricular pressure-volume relations by miniaturized conductance micromanometry. *Am. J. Physiol.* **274,** H1416–1422 (1998).

185. Pacher, P., Nagayama, T., Mukhopadhyay, P., Bátkai, S. & Kass, D. A. Measurement of cardiac function using pressure-volume conductance catheter technique in mice and rats. *Nat. Protoc.* **3,** 1422–1434 (2008).

186. Michael, L. H. *et al.* Myocardial ischemia and reperfusion: a murine model. *Am. J. Physiol.* **269,** H2147–2154 (1995).

187. Patten, R. D. *et al.* Ventricular remodeling in a mouse model of myocardial infarction. *Am. J. Physiol.* **274,** H1812–1820 (1998).

188. Bialik, S. *et al.* Myocyte apoptosis during acute myocardial infarction in the mouse localizes to hypoxic regions but occurs independently of p53. *J. Clin. Invest.* **100,** 1363–1372 (1997).

189. Rockman, H. A. *et al.* Segregation of atrial-specific and inducible expression of an atrial natriuretic factor transgene in an in vivo murine model of cardiac hypertrophy. *Proc. Natl. Acad. Sci. U. S. A.* **88,** 8277–8281 (1991).

190. Rockman, H. A., Wachhorst, S. P., Mao, L. & Ross, J., Jr. ANG II receptor blockade prevents ventricular hypertrophy and ANF gene expression with pressure overload in mice. *Am. J. Physiol.* **266,** H2468–2475 (1994).

191. Patten, R. D. *et al.* 17 Beta-estradiol differentially affects left ventricular and cardiomyocyte hypertrophy following myocardial infarction and pressure overload. *J. Card. Fail.* **14,** 245–253 (2008).

192. Arber, S. *et al.* MLP-deficient mice exhibit a disruption of cardiac cytoarchitectural organization, dilated cardiomyopathy, and heart failure. *Cell* **88,** 393–403 (1997).

193. Kubota, T. *et al.* Dilated cardiomyopathy in transgenic mice with cardiac-specific overexpression of tumor necrosis factor-alpha. *Circ. Res.* **81,** 627–635 (1997).

194. Kubota, T. *et al.* Soluble tumor necrosis factor receptor abrogates myocardial inflammation but not hypertrophy in cytokine-induced cardiomyopathy. *Circulation* **101,** 2518–2525 (2000).

195. Li, Y. Y. *et al.* Myocardial extracellular matrix remodeling in transgenic mice overexpressing tumor necrosis factor alpha can be modulated by anti-tumor necrosis factor alpha therapy. *Proc. Natl. Acad. Sci. U. S. A.* **97,** 12746–12751 (2000).

196. Satoh, M. *et al.* Requirement of Rac1 in the development of cardiac

hypertrophy. *Proc. Natl. Acad. Sci. U. S. A.* **103,** 7432–7437 (2006).

197. Sussman, M. A. *et al.* Altered focal adhesion regulation correlates with cardiomyopathy in mice expressing constitutively active rac1. *J. Clin. Invest.* **105,** 875–886 (2000).

198. Satoh, M. *et al.* Requirement of Rac1 in the development of cardiac hypertrophy. *Proc. Natl. Acad. Sci. U. S. A.* **103,** 7432–7437 (2006).

199. Sawada, N., Salomone, S., Kim, H.-H., Kwiatkowski, D. J. & Liao, J. K. Regulation of endothelial nitric oxide synthase and postnatal angiogenesis by Rac1. *Circ. Res.* **103,** 360–368 (2008).

200. Orr, A. W. *et al.* Matrix-specific p21-activated kinase activation regulates vascular permeability in atherogenesis. *J. Cell Biol.* **176,** 719–727 (2007).

201. Tan, W. *et al.* An essential role for Rac1 in endothelial cell function and vascular development. *FASEB J. Off. Publ. Fed. Am. Soc. Exp. Biol.* **22,** 1829–1838 (2008).

202. Knezevic, I. I. *et al.* Tiam1 and Rac1 are required for platelet-activating factor-induced endothelial junctional disassembly and increase in vascular permeability. *J. Biol. Chem.* **284,** 5381–5394 (2009).

203. Greco, C. M. *et al.* Chemotactic effect of prorenin on human aortic smooth muscle cells: a novel function of the (pro)renin receptor. *Cardiovasc. Res.* **95,** 366–374 (2012).

204. Bond, M., Wu, Y.-J., Sala-Newby, G. B. & Newby, A. C. Rho GTPase, Rac1, regulates Skp2 levels, vascular smooth muscle cell proliferation, and intima formation in vitro and in vivo. *Cardiovasc. Res.* **80,** 290–298 (2008).

205. Laudanna, C., Campbell, J. J. & Butcher, E. C. Role of Rho in chemoattractant-activated leukocyte adhesion through integrins. *Science* **271,** 981–983 (1996).

206. De las Fuentes, L., Yang, W., Dávila-Román, V. G. & Gu, C. C. Pathway-based genome-wide association analysis of coronary heart disease identifies biologically important gene sets. *Eur. J. Hum. Genet. EJHG* **20,** 1168–1173 (2012).

207. Ferri, N., Corsini, A., Bottino, P., Clerici, F. & Contini, A. Virtual screening approach for the identification of new Rac1 inhibitors. *J. Med. Chem.* **52,** 4087–4090 (2009).

208. Irwin, J. J. & Shoichet, B. K. ZINC--a free database of commercially available compounds for virtual screening. *J. Chem. Inf. Model.* **45,** 177–182 (2005).

209. Morris, G. M. *et al.* AutoDock4 and AutoDockTools4: Automated docking with selective receptor flexibility. *J. Comput. Chem.* **30,** 2785–2791 (2009).

210. Ruffoni, A. *et al.* 2-Amino-3-(phenylsulfanyl)norbornane-2-carboxylate: An Appealing Scaffold for the Design of Rac1-Tiam1 Protein-Protein Interaction Inhibitors. *J. Med. Chem.* (2014). doi:10.1021/jm401924s

211. Brown, L. F. *et al.* Expression and distribution of osteopontin in human tissues: widespread association with luminal epithelial surfaces. *Mol. Biol. Cell* **3,** 1169–1180 (1992).

212. Ferri, N. *et al.* Proprotein convertase subtilisin kexin type 9 (PCSK9) secreted by cultured smooth muscle cells reduces macrophages LDLR levels.

Atherosclerosis **220,** 381–386 (2012).

213. Von Wnuck Lipinski, K. *et al.* Integrin-mediated transcriptional activation of inhibitor of apoptosis proteins protects smooth muscle cells against apoptosis induced by degraded collagen. *Circ. Res.* **98,** 1490–1497 (2006).

214. Ferri, N. *et al.* 3-Aryl-N-aminoylsulfonylphenyl-1H-pyrazole-5-carboxamides: a new class of selective Rac inhibitors. *MedChemComm* **4,** 537–541 (2013).

215. Blangy, A. *et al.* TrioGEF1 controls Rac- and Cdc42-dependent cell structures through the direct activation of rhoG. *J. Cell Sci.* **113 (Pt 4),** 729–739 (2000).

216. Michiels, F., Habets, G. G., Stam, J. C., van der Kammen, R. A. & Collard, J. G. A role for Rac in Tiam1-induced membrane ruffling and invasion. *Nature* **375,** 338–340 (1995).

217. Abe, K. *et al.* Vav2 is an activator of Cdc42, Rac1, and RhoA. *J. Biol. Chem.* **275,** 10141–10149 (2000).

218. Del Pozo, M. A. *et al.* Integrins regulate Rac targeting by internalization of membrane domains. *Science* **303,** 839–842 (2004).

219. Montalvo-Ortiz, B. L. *et al.* Characterization of EHop-016, novel small molecule inhibitor of Rac GTPase. *J. Biol. Chem.* **287,** 13228–13238 (2012).

220. Montalvo-Ortiz, B. L. *et al.* Characterization of EHop-016, novel small molecule inhibitor of Rac GTPase. *J. Biol. Chem.* **287,** 13228–13238 (2012).

221. Shutes, A. *et al.* Specificity and mechanism of action of EHT 1864, a novel

small molecule inhibitor of Rac family small GTPases. *J. Biol. Chem.* **282,** 35666–35678 (2007).